Title
ON THE PLASTIC BEHAVIOR OR POLYCRYSTALLINE AGGREGATES

Authors
Dorn, John E.
D, Jim
Mote

Publication Date
1962-03-01

UCRL-10152

University of California

Ernest O. Lawrence Radiation Laboratory

Berkeley, California

DISCLAIMER

Presented at the Research Conference on Structure and Properties of Engineering Materials, North Carolina - March 1962. (to be published)

UCRL-10152

UNIVERSITY OF CALIFORNIA
Lawrence Radiation Laboratory
Berkeley, California

Contract No. W-7405-eng-48

ON THE PLASTIC BEHAVIOR OF POLYCRYSTALLINE AGGREGATES

John E. Dorn and Jim D. Mote

March, 1962

I. INTRODUCTION

One of the major objectives of physical metallurgy is the rationalization of the plastic behavior of metals in terms of the atomistic mechanisms of single crystal deformation. As a result of the basic scientific importance as well as the technical significance of this subject, an extensive literature has developed and numerous surveys[1, 2, 3] have already been made on various aspects of metal plasticity. It is now recognized that four major processes are responsible for deformation in crystalline aggregates: (1) crystallographic glide, (2) twin formation, (3) grain boundary shearing, and (4) stress-directed diffusion of vacancies. Stress-directed diffusion of vacancies contributes significantly to creep straining of polycrystalline materials only at low stresses and at temperatures approaching the melting points[4] for polycrystalline materials that exhibit numerous glide systems (e.g., F.C.C. metals) grain boundary shearing is usually restricted to temperatures above about one-half of the melting temperature where creep is controlled by the climb of dislocations. On the other hand in systems (e.g., Hex. C.P. such as Mg) which have only relatively few operative glide systems grain boundary shearing has been observed at temperatures as low as 78°K.[5] Although twinning may be induced in many metals, the deformations that can be achieved by this mechanism are limited geometrically.[6] Crystallographic glide qualifies as the principal process of deformation in F.C.C. metals at low and intermediate temperatures. Twinning indeed affects in a major way the strain hardening that is observed as a result of interferences to slip but precise knowledge on this aspect is meagre. From this point of view it is reasonable to attempt to limit this discussion principally to examples of plastic def-

ormation by slip in F. C. C. metals. Such a limitation is further justified by the fact that most of the currently available research results on mechanisms of deformation and analyses of strain hardening have been made on F. C. C. metals at low temperatures.

Although the mechanical behavior of aggregates of several phases might be included in a general discussion of the behavior of polycrystalline materials, this subject is indeed a separate chapter, involving the introduction of additional concepts and it will therefore be excluded from the present review.

The plastic behavior of polycrystalline metals appears to be somewhat different from that exhibited by individual single crystals. Frequently, polycrystalline metals have about the same rates of strain hardening as single crystals undergoing multiple slip, but their flow stresses are invariably somewhat higher than those for single crystals; the flow stress increases linearly with the reciprocal of the square root of the grain diameter. In the past it has generally been assumed that, at least in the absence of grain boundary shearing, the basic mechanisms of deformation in single and polycrystalline metals are the same. If this were so, the behavior of polycrystalline aggregates could be deduced from a complete knowledge of single crystal behavior. We will, therefore, consider in the next sections (II, III and IV) the status of our knowledge on single crystal behavior and in the section V the behavior of bicrystals, which begin to approach more closely the behavior of polycrystals. In section VI we will demonstrate that the existing attempts to deduce the behavior of polycrystalline aggregates in terms of the behavior of single crystals suggests that the flow stresses are only a few times greater than those for single crystals and are independent of grain size. Undoubtedly, new factors not inherent in single crystal deformation enter the picture. These will be discussed in section VII. We

will show that, in contrast to the usual assumptions of homogeneous deformation by multiple slip, deformation is highly localized. Consequently, dislocations pile up against the boundaries of unfavorably oriented grains and depending on their relative orientations either produce slip on the usual slip planes or on uncommon planes only operative in polycrystals. The stresses at the head of piled-up arrays depend in such a way on grain size that the flow stress becomes proportional to the reciprocal of the square root of the grain diameter. The plastic behavior of polycrystals therefore cannot be deduced exclusively from single crystal data because new factors, such as heterogeneous behavior, new slip mechanisms and piled-up arrays of dislocations, enter the picture. More effort must therefore be devoted directly toward understanding these auxiliary features of the deformation in polycrystalline metals.

II. THEORIES OF SINGLE CRYSTAL BEHAVIOR

Although some aspects of the theory of the plastic behavior of single metal crystals are yet under discussion, there is general agreement relative to the shape of experimentally determined stress-strain curves.[1, 2, 3] In Fig. 1 are shown the resolved shear stress versus resolved shear strain curves for Cd (0001) $[11\bar{2}0]$ [7], Al $(11\bar{1})$ $[10\bar{1}]$ [8], and Cu $(11\bar{1})$ $[10\bar{1}]$ [9] for the temperatures and orientations indicated.

Whereas the Cd (Hex. C. P.) crystals exhibit only a modest amount of strain hardening over the entire range of deformation, the Cu and Al crystals have an initial range, Stage I, of mild linear hardening (also known as easy glide), a Stage II of rapid linear strain hardening, and a Stage III over which the rate of strain hardening decreases. The low rate of strain hardening over Stage I in the F. C. C. metals approximates that for Hex. C. P. metals insofar as it suggests substantially unperturbed slip on the principal slip system. Over this region the slip bands are usually continuous

over the entire crystal surface. Over Stage II, however, the principal slip bands become progressively shorter[9, 10, 11, 12] implying that some interference to easy glide takes place. The absence of Stage II in Hex. C. P. metals reveals that the mechanism of hardening in Stage II is uniquely associated with the multiplicity of possible operative slip systems in F. C. C. metals leading to blockage of slip on the principal slip plane. The lower strain-hardening rate that is observed over Stage III must be ascribed to some process that allows a moderation of the higher rate of strain-hardening operative earlier over Stage II. It has been shown that the reduced rate of strain hardening in Stage III arises from the stress assisted thermal activation of cross-slip.[2]

Stages I and II of the low temperature plastic behavior of F. C. C. metals has been ascribed to an intersection model which was introduced by Mott[13] and Cottrell[14] and extended in detail by Friedel[15] and Seeger[16]. According to the general assumptions of this model the interruptions of easy glide at the terminus of Stage I was ascribed to the formation of Lomer-Cottrell sessile dislocation blocks produced by reactions of the form

$$a/2\,[101]_{(11\bar{1})} + a/2\,[01\bar{1}]_{(111)} \longrightarrow a/6\,[110]_{(001)} + a/6\,[11\bar{2}]_{(11\bar{1})} + a/6\,[11\bar{2}]_{(111)} \quad (1)$$

Since the energy decreases a stable sessile arrangement is obtained of dislocations lying on the three designated planes. Thus, two stacking faults are formed on the $(11\bar{1})$ and the (111) planes, respectively, which issue from the $a/6\,[110]$ dislocation and terminate at the two partial dislocations. On the basis of electron microscopical evidence,[10] which reveals that

continuously decreasing lengths of slip bands are produced during the same interval of deformation as the shear strain increases, Seeger concludes that the formation of Lomer-Cottrell dislocations continues throughout Stage II. The theory further postulates that dislocations on the primary slip system pile up against the Lomer-Cottrell sessile dislocations producing in this way long-range back stresses. The energy that is required to move dislocations against such long range stress fields is very large and consequently this process is not thermally activatable. Therefore, the component of the flow stress necessary to overcome the long range stress fields is substantially independent of the temperature. As the dislocations move away from their Frank-Read sources, however, they must intersect dislocations of the Frank network that thread through the slip plane; thus, they form jogs. The energy for intersection depends on the geometric details of the process as well as the stacking fault energy. But estimates of these energies for intersection usually range from a fraction to several electron volts and therefore the intersection process is thermally activatable. Consequently, the flow stress, τ, must equal the temperature insensitive long-range back stress, τ_G^*, plus the temperature dependent activation stress, τ_i, necessary for intersection. The initiation of Stage III is attributed to the nucleation of cross-slip among the highly stressed leading dislocations in the piled-up arrays. Since cross-slip is thermally activatable, the stress $\tau_{II,\ III}$ must decrease with increasing temperatures as shown in Fig. 2[12]

Although this theory has been reasonably successful in accounting for the observed plastic behavior of single F.C.C. metal crystals, recently documented evidence, primarily that which has been obtained by transmission electron microscopy has cast doubts on the validity of several major assumptions that were made. Much of this evidence was discussed at the Fifth General Assembly of the International Union of Crystallography (University

of Cambridge, August, 1960). And a preliminary analysis of the newer concepts was reported by Mott in the 1960 Institute of Metals Lecture.[17] The critical observations, primarily due to Hirsch, are as follows:

1. Although detailed searches have been made there is not direct transmission electron microscopical evidence for the formation of Lomer-Cottrell dislocations. Stroh[18] has shown that, under sufficiently high stresses, the Lomer-Cottrell dislocations, particularly in high-stacking-fault energy metals, can be made to dissociate under the stress fields of piled-up dislocation arrays. Furthermore, Kochs[19] has shown that the incidence of formation of Lomer-Cottrell dislocations should indeed be small.

2. Piled-up arrays of dislocations are seen in low stacking fault energy metals and also at the grain boundaries in various polycrystalline metals. On the other hand no well defined numerous pile-ups have been seen in the grain centers of Al and Cu crystals.

3. In lieu of pile-ups, straining into Stage II causes the formation of networks of severely entangled dislocations within which there are practically no free dislocations.

4. Generally much "debris" including vacancies, is left along the trail of a moving dislocation. The motion of dislocations is arrested at jogs, and dislocation loops are frequently left behind the trails of superjogs.

As mentioned by Mott, Hirsch has shown that whereas interstitial jogs move conservatively along the length of screw dislocations, it is easier for vacancy jogs to leave a trail of vacancies in their wake. On this basis Hirsch postulates that the major cause for strain hardening arises from this mechanism. If the temperature is sufficiently high that vacancies can diffuse away the activation energy for slip becomes $U_{SD} - L_v \tau b^2$ where U_{SD} is the activation energy for self-diffusion, τ is the applied stress, L_v is the distance between vacancy jogs and b is the Burger's vector. But at

lower temperatures, where diffusion is too slow, the vacancy trail produces a back force on the dislocations which must be overcome exclusively by the applied stress and the behavior is athermal. Therefore, the stress necessary to cause deformation at low temperatures is given by

$$\tau L_v b^2 = \alpha G b^3 \qquad (\alpha \simeq 0.2) \tag{2}$$

where G is the shear modulus of elasticity and $\alpha G b^3$ is approximately the energy to produce a vacancy. The estimated value of τ is slightly below that given by $\tau = Gb/2L_v$ which is required to cause the dislocation segment between two jogs to behave like a Frank-Read source. Furthermore, the attraction between the dislocation dipoles also prevents the segment from undertaking the Frank-Read mechanism.

By taking into consideration the mutual annihilation of vacancy and interstitial jogs Mott deduces that $L_v \simeq \sqrt{2}L$ where L is the dislocation spacing in the dense region of the forest. The resulting relationship that

$$\tau = \alpha G b / \sqrt{2} L \tag{3}$$

is in good agreement with the experimentally determined oorrelations of Bailey and Hirsch.[20] This agreement with experiment however is not definitive since a similar relationship results from the postulates of an intersection mechanism.

An essential feature of Mott's theory concerns the relief of back stresses on the primary sources by appropriate motion of dislocations on secondary systems. Mott believes that such motion is responsible for the observed entanglements. The strain $d\gamma$ that is obtained when dn primary dislocations per unit volume move an average distance R from the source

center is given by

$$d\gamma = \pi R^2 b\, dn \tag{4}$$

Dislocations on the secondary slip systems move a fraction g of the motion on the primary system so as to relieve the stresses. But as shown by Cottrell[21] only a fraction f (equal to about 1/20) of the jogs produced by intersection of the primary dislocations will be vacancy jogs. Therefore, the number of vacancy jogs produced per unit length of the primary dislocations, dm_v, by the stress-relief motion of the secondary dislocations is given by

$$dm_v = g f \pi R^2 dn \tag{5}$$

This follows from the fact that a single dislocation moving through an area A of a forest of density ρ produces ρA jogs on these dislocations and therefore the jogs produced per unit length are merely A. Consequently, from Eqn. (2), (4) and (5)

$$\frac{d\tau}{d\gamma} = \alpha G b \frac{dm_v}{d\varepsilon} = \alpha G b \frac{g f \pi R^2 dn}{\pi R^2 b\, dn} = \alpha g f G \tag{6}$$

or

$$\tau = \alpha g f G (\gamma - \gamma_0)$$

where γ_0 is the strain for the beginning of Stage II. Comparing with the experimentally determined value of

$$\left(\frac{1}{G}\right)\left(\frac{d\tau}{d\gamma}\right) \simeq \frac{1}{300}$$

for Stage II, reveals that g has the acceptable value of about 1/3.

Seeger et al[9] have shown that the lengths of dislocation segments visible on the surface of incrementally strained crystals decreases progressively as the strain increases. Mott suggests that these lengths are about equal to 2 R the diameter of the entanglement. To obtain an estimate of such lengths Mott rewrites Eqn. (3) in terms of the density, ρ, of dislocations in the thick part of the forest as

$$\tau^2 = \alpha^2 G^2 b^2 \frac{\rho}{2} \tag{7}$$

where

$$d\rho = 2\pi R\, dn = 2\pi R \left(\frac{d\gamma}{\pi R b}\right) = \frac{2\,d\gamma}{Rb} \tag{8}$$

Therefore

$$\tau \frac{d\tau}{d\gamma} = \frac{1}{4} G^2 b^2 \left(\frac{d\tau}{d\gamma}\right) = \frac{1}{4} G^2 b^2 \left(\frac{2}{Rb}\right) = \frac{G^2 b}{2R}$$

Introducing Eqn. (6) gives

$$2R = \frac{G^2 b}{(\alpha g f G)^2 (\gamma - \gamma_0)} = \frac{b}{\alpha g f (\gamma - \gamma_0)} \tag{9}$$

The calculated values are only slightly smaller than the measured values.

Obviously, Mott's analysis for jog hardening is yet in the early developmental stages: 1. The exact details for the formation of entanglements have neither been observed nor calculated. 2. The conservative motion of interstitial jogs has not been confirmed experimentally. 3. And the theory, as it now stands, is at best a preliminary estimate. 4. Many additional considerations are involved as follows: (a) what is the distinction between Stages I, II and III? (b) can quantitative analyses be provided for orientation and size effects? (c) what process accounts for the thermally

activated part of the stress? (d) how does the activation energy depend on stress? (e) can the Cottrell-Stokes ratio be obtained theoretically? (f) what process takes place in Stage III, and (g) what is the activation energy involved? Until these and other pertinent questions are fully answered it will be necessary to withhold final judgement on this mechanism.

Although the jog hardening mechanism appears to have several advantages over the intersection mechanism, Seeger, Mader and Kronmuller[22] continue to assert, with considerable authority, that the major concepts of the intersection mechanism are yet correct: 1. The dislocation arrangements in cold worked metals distinctly represent non-equilibrium conditions. As thin films are produced from bulk material, dislocations must undertake re-arrangements due to removal of dislocations eliminated in the preparation of the thin foil. Remaining dislocations react to their now strong image forces. 2. Electron microscopic investigations on active slip line traces give rather directly those quantities which are important for quantitative dislocation models of work hardening, namely slip distances of dislocation, sizes of dislocation groups, and the crystallography of glide. These observations agree in detail with the precepts of the intersection model. 3. Ferromagnetic saturation measurements, which definitely pertain to the bulk material, unambiguously reveal the presence of long range back stresses over distances between 50 and 500 Å and thus give quantitative confirmation of the increasing presence of long range stresses over deformations in Stage II. These arguments, in favor of the intersection model, are further strengthened by (a) the now established failure of the constancy of the Cottrell-Stokes ratio[23] which demands independent long and short range stress fields, and (b) by the dependency of the activation energy on the stress and stacking fault width in a way that is consistent with the intersection mechanism. From these viewpoints only two kinds of electron microscopical observations remain to embarrass the unqualified acceptance of the intersection model.

The first pertains to the absence of Lomer-Cottrell dislocations. However, Lomer-Cottrell dislocations are not essential to the acceptance of the intersection mechanism. Any suitable origin of long range back stresses will suffice; and such back stresses can well arise from entangled dislocation networks. The second issue concerns the presence of trailing jogs and loop debris. These also could contribute to the athermal back stresses.

III. ANALYSES OF EXPERIMENTAL DATA

The ultimate acceptance of any theory describing the plastic behavior of single crystals will eventually depend on its ability to account analytically for all of the experimental facts. We, therefore, propose to review briefly some of the principal observations that have been made. The analyses can be couched in such general terms that they might apply to any acceptable detailed model. On the other hand it will prove convenient to use the special terminology that has been developed for the intersection model. We, therefore, adopt Seeger's expression for the plastic strain rate, $\dot{\gamma}$, when the deformation is controlled by a single thermally activated process, namely,

$$\dot{\gamma} = N A b \nu e^{-\frac{U}{kT}} \tag{10}$$

where N is the number of points per cm^3, at which activation can occur, A is the area swept out per activation, b is the Burger's vector, ν is the frequency (usually about the Debye frequency), U is the energy that need be supplied by a thermal fluctuation for each successful activation. In general, U will depend on the local stress and the details of the mechanism. If L is the mean cord distance between neighboring points at which the dislocation is arrested, the net force, F, due to the line tension of the dislocations, acting at this point is

$$F = (\tau - \tau^*) L b \tag{11}$$

where τ is the externally applied stress and τ^* is the back stress not surmountable by a thermal fluctuation. Thus, in general, as suggested by Basinski,[24] the activation energy, for the process can be represented, as shown in Fig. 3 by

$$U = \int_{F=(\tau-\tau^*)Lb}^{F_m} x\, dF \tag{12}$$

The experimentally determined F-x curve may provide critical criterion for the selection of the operative model for thermal activation of glide.

Two experimental observations are required to obtain the F-x curve. For one we define

$$\beta = \left(\frac{\partial \ln \dot{\gamma}}{\partial \tau}\right)_T = \frac{x L b}{kT} \tag{13}$$

which follows directly from Eqns. (10), (11) and (12). The experimentally determined values of the activation volume, $xLb = \beta kT$ for Cu are shown in Fig. 4 as a function of the flow stress τ_T (at the test temperature T). The second type of required data for the determination of the F-x curve consists of the Cottrell-Stokes ratio τ_T / τ_{77} which is given for Cu as a function of the flow stress at 77°K in Fig. 5. We note here that this ratio is not a constant but depends on the work-hardened state as well as the temperature. If we write the integral of Eqn. (12) as $\varphi\{(\tau-\tau^*)Lb\}$ introduce this value into Eqn. (10), and solve explicitly for the flow stress τ we obtain

$$\tau = \tau^* + \frac{1}{Lb}\varphi^{-1}\left\{kT \ln \frac{NAbv}{\dot{\gamma}}\right\} \tag{14}$$

$$F = (\tau - \tau^*) L b \tag{11}$$

where τ is the externally applied stress and τ^* is the back stress not surmountable by a thermal fluctuation. Thus, in general, as suggested by Basinski,[24] the activation energy, for the process can be represented, as shown in Fig. 3 by

$$U = \int_{F=(\tau-\tau^*)Lb}^{F_m} x\, dF \tag{12}$$

The experimentally determined F-x curve may provide critical criterion for the selection of the operative model for thermal activation of glide.

Two experimental observations are required to obtain the F-x curve. For one we define

$$\beta = \left(\frac{\partial \ln \dot{\gamma}}{\partial \tau}\right)_T = \frac{xLb}{kT} \tag{13}$$

which follows directly from Eqns. (10), (11) and (12). The experimentally determined values of the activation volume, $xLb = \beta kT$ for Cu are shown in Fig. 4 as a function of the flow stress τ_T (at the test temperature T). The second type of required data for the determination of the F-x curve consists of the Cottrell-Stokes ratio τ_T / τ_{77} which is given for Cu as a function of the flow stress at 77°K in Fig. 5. We note here that this ratio is not a constant but depends on the work-hardened state as well as the temperature. If we write the integral of Eqn. (12) as $\varphi\{(\tau-\tau^*)Lb\}$ introduce this value into Eqn. (10), and solve explicitly for the flow stress τ we obtain

$$\tau = \tau^* + \frac{1}{Lb}\varphi^{-1}\left\{kT \ln \frac{NAb\nu}{\dot{\gamma}}\right\} \tag{14}$$

where the final term represents the stress required to aid the thermally activated process. The failure of the Cottrell-Stokes ratio to remain constant over a range of work hardened states clearly reveals that τ^* does not vary exclusively as the short range field which is proportional to 1/L, other factors being about the same. Consequently, the thought, previously expressed by Basinski, that the back stress arises exclusively from more localized interactions of the stress fields of intersecting dislocations is untenable.[23] The value of τ^* as will be shown later, arises from the sum of the local stresses and the long range back stresses. It is also equally difficult to account for this experimental fact in terms of the jog mechanism for strain hardening as proposed by Mott. Necessarily, the work hardened state must be identified in terms of at least two quantities such as τ^* and L.

Since μ and τ^* both depend on the temperature through the shear modulus of elasticity it is necessary to refer to the F_o-x curve at the absolute zero of temperature. Therefore, Eqn. (11) will be rewritten as

$$\tau L b G_o/G = F_o + \frac{\tau^* G_o L b}{G} = F_o + \tau_o^* L b \qquad (15)$$

the subscripts zero referring to the values at the absolute zero of temperature. Thus, we see that the value of $\tau L b G_o/G$ for a given work hardened state (i.e., constant values of τ_o^* and L) differs by a constant, namely $\tau_o^* L b$ from the desired value of F_o. To arrive eventually at $\tau L b G_o/G$ we first plot $\tau G_o/G$ as a function of $\beta kT = \chi L b$ as shown in Fig. 6. Each solid line was obtained for a given strain hardened state as identified by the flow stress at 77°K and strain rate adjusted to $\dot{\gamma} = 15 \times 10^{-6}$/sec. by means of the Cottrell-Stokes ratio and the values of βkT are obtained for the corresponding state from

Fig. 4. The broken lines connect points for various strain-hardened states obtained under constant conditions of $\dot{\gamma}$ and T. Along each of the solid lines, τ^* and L are constant; and along each of the broken lines, neglecting in small effect of changes in NA in Eqn. (10), U_o is a constant. Consequently, as shown by Eqns. (12) and (15), F_o and x are constant along the broken curves. Therefore, the decreasing values of $\chi L b$ with increasing values of $\tau G_o/G$ along the broken curve is exclusively due to the decrease of L with strain hardening.

As shown by Eqn. (10) the activation energy for a given $\dot{\gamma}$ vanishes as the temperature approaches the absolute zero. Thus, at 4°K most of the work necessary to overcome the effective barrier is done by the applied stress. Under these conditions the distance x that the dislocation is moved must approximate the shortest possible distance, i. e., about one Burger's vector for intersection or motion of a jog. Therefore, along the broken line for 4°K

$$\beta kT = \chi L b \simeq L b^2$$

In this way the value of L for each work hardened state can be obtained. And since L remains constant along any solid curve the value of x can be obtained for each point in Fig. 6. Thus, the approximate $\tau G_o L b/G$ versus x curve can be established for each work-hardened state as shown in Fig. 7. It is significant that, in agreement with the dictates of Eqn. (15), the curves for the higher work-hardened states are merely shifted upward, the difference in the ordinates between two curves being equal to the differences of the values of $\tau_o^* L b$ for the two states. Consequently, auxiliary information must be sought to establish the absolute value of τ_o^* as a function of the strain-hardened state.

For the intersection mechanism τ_o^* arises from at least two

sources: (a) the stress, τ_{oi}^* necessary to overcome the interaction of the intersection dislocations, and the stress, τ_{ol}^* due to long range stress fields arising from dislocations lying approximately parallel to the moving dislocation. At the initial yield strength the latter should indeed be negligible. Saada[25] estimates that the average value of τ_{oi}^* is about

$$\tau_{oi}^* L b = \alpha G_o b^2 \qquad (16)$$

At the initial yielding for the highest temperature that was employed, the stress necessary to aid the thermal fluctuation is small, and consequently the flow stress equals about τ_{oi}^*. This suggests that $\alpha \simeq 0.046$, a value of about 1/4 that originally estimated by Saada. The differences in the ordinates of Fig. 7 refer to differences in $\tau_{ol}^* L b$, which has a value near zero for the yield stress curve. The values of τ_{ol}^* obtained in this way are given as a function of the strain at 77°K in Fig. 8. The variation of τ_{oi}^* and 1/L with strain are also represented in the same figure. Over Stage I, 1/L increases only slightly with strain whereas over Stage II it increases more rapidly with strain. On the other hand τ_{ol}^* increases almost parabolically with the strain over Stage II. Thus, the trends in τ_{oi}^* and τ_{ol}^* reveal a distinct difference between the short range fields and the long range stress fields, in a sharp contrast with deductions based on Mott's model.

Subtracting $\tau_o^* L b$ from $\tau L b G_o/G$ gives the F_o-x diagram shown in Fig. 9. A similar analysis for Al provides the broken curve in Fig. 9. On the basis of the intersection model the differences between the curves for Cu and Al could be attributed to the greater energy for producing a constriction in Cu, where the partials are more widely separated than in Al. It is difficult, however, to understand the origin

of these differences in terms of jog-hardening model as set down by Mott. Additional evidence in favor of the intersection model have recently been reviewed by Seeger, Mader, and Kronmuller.[22] We, therefore, conclude that current evidence strongly supports the validity of the intersection model.

IV. ORIENTATION EFFECTS AND INFLUENCE OF OTHER FACTORS

Although extensive investigations have been made on the effect of orientation on the plastic behavior of single crystals, up to the present no detailed analyses, such as those given in the preceeding discussion, are yet available. Nevertheless, the phenomenological observations of orientation effects have important implications relative to the behavior of polycrystalline aggregates. Therefore, these factors, which have been reviewed in detail by Clarebrough and Hargreaves,[1] will be briefly summarized here.

Typical results on the effect of orientation on the stress-displacement curves for single crystals are given in Fig. 10[26, 27] In general, the following conclusions are obtained: (a) The shapes of the stress-strain curves are sensitive to orientation. (b) As the orientation approaches the [001] to [111] line of the standard triangle, the extent of easy glide is reduced. Thus, the nearer the orientation is to that under which duplex slip will occur, the shorter is easy glide. This suggests that slip on the secondary planes introduce barriers to slip that terminate easy glide. (c) The rate of strain hardening during easy glide also increases as the crystal axis approaches the [001] to [111] boundary of the standard triangle suggesting that some slip on the secondary slip planes takes place somewhat before the idealized orientation for duplex slip is reached. (d) As the orientation approaches the [001] to [111] line, the rate of strain hardening for Stage II also increases but not as much as for Stage I. (e) Rossi[28] as well as Suzuki et al[29] have shown that the greatest rates of strain hardening for Stage II are obtained for orientations near the [001] poles where ideally eight slip

mechanisms can become operative. (f) The initiation of Stage III is not, in general, sensitive to orientation. (g) But, as shown in Fig. 11[30] orientations in the immediate vicinity of the [111] pole exhibit higher rates of strain hardening for Stage III than orientations in the immediate vicinity of the [001] pole.

Other factors also influence the behavior of the stress-strain curves for single crystals: (a) The extent of easy glide decreases as the temperature increases and it increases with additions of impurities and alloying elements. This is thought to arise from the Cottrell and Suzuki locking which would restrain slip on the secondary planes. (b) Larger crystals exhibit shorter regions of easy glide either due to the greater chance of motion of dislocations on secondary systems or to the greater probability of forming Lomer-Cottrell dislocations. (c) Precipitates decrease the extent of easy glide. (d) Plated layers appear to reduce the extent of easy glide. (e) Torsional straining increases the flow stress and the rate of strain hardening under subsequent tension conditions. (f) The range of Stage II decreases with an increase in temperature and it is smaller for such higher stacking fault energy metals as Al when compared with such lower stacking fault energy metals as Cu. (g) The rate of strain-hardening in Stage II is insensitive to the presence of minor amounts of alloying elements, surface conditions and crystal size. (h) Torsional straining causes an immediate increase in the subsequent flow stress in tension, but has practically no effect on the subsequent rate of strain hardening. (i) The rate of strain hardening in Stage II decreases slightly more rapidly than linearly with the shear modulus of elasticity as the temperature increases. (j) The rate of strain hardening in Stage III is lower for the higher test temperatures.

Undoubtedly, each of these factors is significant to the behavior of polycrystalline aggregates. Consequently, any completely satisfactory theory of deformation of polycrystalline metals must adequately include

numerous details pertaining to the behavior of each grain. These observations, in part, reveal the magnitude of the problem and suggest why advances on the important issue of strain hardening are so slow.

V. PLASTIC BEHAVIOR OF BICRYSTALS AND MULTICRYSTALS HAVING VERTICAL GRAIN BOUNDARIES

The plastic behavior of polycrystalline aggregates must arise from two factors: (a) the slip processes that occur in each individual and dissimilarly oriented grain, and (b) the effects introduced by the grain boundaries. In the preceeding section we have observed that even the plastic behavior of single crystals depends on their orientation. In particular, those orientations which are more favorably oriented for slip on a secondary system give smaller amounts of easy glide, higher work-hardening rates over Stage I and somewhat higher rates of work hardening over Stage II. This occurs even when the resolved shear stress on the secondary system is less than the expected critical value for duplex slip and even when the amount of slip on secondary systems is negligibly small. Undoubtedly, This effect persists in a pronounced way in polycrystalline aggregates. But, additional factors such as continuity of deformation across grain boundaries usually demand the simultaneous operation of as many as five slip systems in a single grain for the general case. Therefore, the stress-strain curve for a grain in the polycrystalline aggregate must differ from that obtained for a given single crystal, even when their orientations relative to the tensile axis are the same. This has led Chalmers[31] to conclude that "any attempt to account in detail for polycrystalline plasticity (exclusively) in terms of the simple slip process is unlikely to be completely successful".

Obviously, the grain boundaries per se play a significant role in determining the plastic behavior of polycrystalline aggregates under con-

ditions where grain boundary shearing becomes significant. It was thought, that grain boundaries might also affect the plastic behavior of polycrystalline metals, even in the absence of grain boundary shearing, by providing a highly viscous strong layer between the grains. If, for example, the atoms in the boundary were highly random and the grain boundary were wide, dislocations might encounter difficulties in traversing this region. But estimates reveal that the grain boundary region is only about five atoms thick and represents a region of transition between the orientation of the two adjacent grains. Furthermore, dislocations usually originate preferentially either in the immediate vicinity of or at the grain boundary itself. Thus, it appears unlikely that the grain boundaries per se in pure metals can provide substantial strengthening of polycrystalline aggregates.

It is quite difficult to arrive at unambiguous decisions on the questions of orientation strengthening effects from direct investigations on polycrystalline aggregates themselves. Much progress has been made, however, in an evaluation of the importance of these factors in polycrystalline metals from experimental studies on the plastic behavior of bi- and multi-crystalline specimens having grain boundaries coincident with the tensile axis.

Livingston and Chalmers[32] have shown that the compatibility of the strains at the grain boundary of a bicrystal constitutes one of the most important factors in rationalizing the plastic behavior of bicrystals. To present this viewpoint we consider the bicrystal of Fig. 12 composed of grains A and B having a mutual boundary in the X-Z plane, Z being the axis of tensile straining. When the grains remain contiguous, the compatibility conditions for the strains ε_{ij} at the boundary, namely

$$\varepsilon_{ZZ}^{A} = \varepsilon_{ZZ}^{B}, \quad \varepsilon_{XX}^{A} = \varepsilon_{XX}^{B}, \quad \varepsilon_{XZ}^{A} = \varepsilon_{XZ}^{B} \qquad (17)$$

must apply. When the conditions of Eqn. (17) also apply to each individual

grain of the bicrystal when tested separately, the orientations are said to be compatible. But if the conditions required by Eqn. (17) do not apply when grains A and B are tested independently the orientation of crystal B relative to A is said to be incompatible. The conditions of compatibility as defined above refer only to the macroscopic average strains at the grain boundary and do not take into consideration the heterogeneity of slip. Thus, provided the presence of the grain boundary per se has no influence on the plastic behavior of bicrystals and the heterogeneities of slip have a negligible effect, the plastic behavior of compatible bicrystals should be simply related to the behavior of the individual grains.

Several investigators have now shown that compatible isoaxial bicrystals do indeed give stress-strain curves that coincide, within experimental scatter, to those of the individual single crystals. Typical results from the recent investigations of Fleischer and Backofen[33] on Al bicrystals are given in Fig. 13. In both Type "a" and Type "b" bicrystals the normal to the slip plane of both crystals A and B made an angle of 90 - χ to the tensile axis. In the Type "a" bicrystals the $[\bar{1}0\bar{1}]$ slip directions were also at 45° to the tensile axis whereas in the Type "b" bicrystal the $[10\bar{1}]$ directions (but not the operative slip directions) were at 90° to the tensile axis. Both bicrystals are isoaxial since grains A and B of each bicrystal are similarly oriented with respect to the Z axis of tensile straining. Furthermore, they are also compatible. The agreement between the stress-strain curves of the compatible isoaxial bicrystals with those for similarly oriented single crystals is excellent. The minor deviations from exact coincidence might easily be due to the commonly observed scatter in the behavior of single and bicrystals and also to the small deviations that must have been present from the ideal compatible-isoaxial orientations.

The high angle boundary in the Type "a" bicrystal might be visualized as composed of a vertical arrangement of edge dislocations. For the

geometry involved, however, the shear stresses arising from possible piled-up arrays of dislocations at the boundary in one grain would promote slip in both grains. Consequently, piled-up arrays should not form, and no boundary effects should be obtained. This deduction is distinctly different from that which applies to low angle boundaries where stresses must be applied to force additional dislocations into the vertical wall of edge dislocations.

In the Type "b" bicrystal dislocations having both edge and screw dislocations must enter the boundary upon deformation. Such dislocations will, as a result of the assumed geometry form a low energy boundary having both tilt and twist components. Here again no interference to dislocations entering the boundary will be encountered.

The identity of the stress-strain curves for isoaxial compatible bicrystals with those for single crystals having the same orientation reveals that neither the boundary per se nor the heterogeneous nature of slip offers any resistance to deformation.

At least four slip mechanisms must operate in the near vicinity of the grain boundary of general incompatible bicrystals. Consider first that Grain "A" of Fig. 12 slips only on one system to provide strains

$$\varepsilon^{A}_{zz}, \quad \varepsilon^{A}_{xx}, \quad \varepsilon^{A}_{xz}$$

In order to satisfy the continuity conditions of Eqn. (17), Grain "B" must experience the same strains at the boundary. When the orientations are compatible, Eqns.(17) are automatically satisfied when only the principal slip system operates in Grain "B". But when the orientations are incompatible other slip systems must operate. Since the strains are linearly related to the slip, at least three independent slip mechanisms must operate in Grain "B" for a general incompatible bicrystal to satisfy Eqns. (17).

Satisfaction of continuity at the grain boundary can also be achieved by the operation of at least two slip systems in each grain. Thus, for the general case at least four slip mechanisms must operate in the vicinity of the boundary in order to preserve continuity. (For special non-compatible orientations only three independent slip systems may be required). Early results on the plastic behavior of incompatible isoaxial bicrystals suggested that both the yield strength and the rate of strain hardening increased with the degree of grain disorientation. All of the more recent studies, conducted under experimental conditions involving more precise extensometry, consistently reveal that the yield strengths of incompatible as well as compatible isoaxial bicrystals coincide extremely well with the yield strength of similarly oriented single crystals.

Aust and Chen[34] investigated bicrystals of Al in which the [011] axis of each crystal coincided with the tensile axis, the differences in orientation being given by the angle θ between the [001] directions in each grain of the bicrystal. Since the [011] direction in cubic crystals is a two-fold axis of symmetry, the plastic properties must vary periodically with a period $\theta = 180^\circ$. The type of stress-strain curve that was obtained is shown in Fig. 14. Our interest will center about the rate of strain hardening $d\sigma/d\varepsilon$ over range AB and the strain ε_θ at which the higher rate of linear hardening was obtained. These data, shown in Fig. 15, reveal that the rate of strain hardening increases and the strain to the point of initiation of rapid linear hardening increases as the disorientation θ between the two grains of the incompatible isoaxial bicrystal increases. These effects must be ascribed to the modifications in strain hardening resulting from the operation of four slip mechanisms in the vicinity of the boundary. A somewhat similar investigation was reported by Clark and Chalmers.[35] They studied the plastic deformation of Al bicrystals, whose orientations are given in Fig. 16 that were so grown as to have common

(coplanar) $\{111\}$ planes. A series of different orientations were obtained by symmetrical rotations of the $[101]$ slip directions of each crystal by angles of plus and minus φ about the $[111]$ axis. Under these conditions the resolved shear stress on the selected planes is identical in both crystals. Since the $[111]$ direction is a three-fold axis of symmetry, the plastic properties must be periodic with rotations of $\theta = 2\varphi = 120^{\circ}$. In general, the yield strength of the bicrystal did not differ materially from that of single crystals having the same orientations. As in the previous example, the rates of strain hardening remained almost linear up to 40% strain; the rate of strain in this region, however, increased with the difference in orientation as shown in Fig. 17.

Fleischer and Backofen[33] have examined the plastic behavior of incompatible-nonisoaxial Al bicrystals. In these cases the yield strength remained approximately that for single crystals, Stage I was absent and the rate of strain hardening was only slightly greater than that for a single crystal undergoing dupiex slip. In conclusion, therefore, the difference in the plastic behavior of single and bicrystals appear to be almost entirely due to the increase in strain hardening rates of the bicrystals resulting from multiple slip in the vicinity of the grain boundary as required to preserve continuity at the boundary.

Detailed investigations on a series of Al bicrystals have been reported by Livingston and Chalmers.[32] As might have been expected, in all of the symmetric, compatible isoaxial crystals that were tested only traces of the one principal $\{111\}$ slip mechanism per grain was observed. Each grain of the sixteen incompatible isoaxial crystals exhibited strong slip markings for the principal $\{111\}$ mechanism on which the resolved applied shear stress was greatest. Furthermore, each such bicrystal exhibited traces of at least one auxiliary mechanism. Some of these slip traces were short being limited to the near vicinity of the boundary. Of these only three

cases were noted where the traces might have originated from slip on {110} planes; all remaining cases could be clearly ascribed to slip on {111} planes.

Livingston and Chalmers also attempted to predict the auxiliary slip mechanisms. Adaptation of Taylor's concept of least energy to the problem of deformation in bicrystals failed to give predictions that coincided with the observations. This is not too surprising since the stress fields due to arrays of dislocations piled up at the boundaries of incompatible bicrystals can exceed many times the applied stress. Therefore, Livingston and Chalmers applied the concept that the auxiliary slip system operative in Grain "B" for example is that on which the resolved shear stress for slip due to the stresses arising from piled-up dislocations on the principal slip plane of A, gives the highest value. Good predications were obtained by this procedure for the limited observations that were made. However, the operative auxiliary planes predicted by this procedure also coincided with those on which the applied shear stress was greatest and consequently the role of piled-up arrays of dislocations in nucleating slip cannot be deduced from this evidence.

We have already noted that as the size of single crystals are increased, the extent of easy glide over Stage I is reduced. Undoubtedly, this effect persists in each grain of a bicrystal. But in incompatible bicrystals the auxiliary rate of strain-hardening due to multiple slip also intervenes to further reduce the easy glide region. Under these circumstances a second size factor arises as a result of the region adjacent to the grain boundary over which the auxiliary slip takes place. Fleischer and Chalmer's investigation of incompatible isoaxial crystals is shown in Fig. 20. They observed that duplex slip extended away from the boundary about the distance equal to the width of the specimen. Thus, whereas duplex slip extended over the entire section of specimen No. 6, it extended over only about 3/4

of specimen No. 7, and about 1/2 of specimen No. 8. Correspondingly, the rate of strain hardening was greatest in the specimens that exhibited the most extensive operation of duplex slip.

In bicrystals, the plastic behavior is affected by the orientation differences at a single boundary. Elbaum[36] has shown that these effects are magnified in specimens composed of three or four grains. He investigated the isoaxial orientation shown in Fig. 19. The crystals were so grown that the slip plane and slip direction were initially at 45° to the tensile axis. The resulting stress-strain curves are shown in Fig. 20. The stress-strain curves of the compatible bi-, tri- and quadru-crystals as well as the incompatible bicrystals fell in the cross-hatched band. Successively higher stress-strain curves were obtained for the incompatible tri- (T) and quadru-crystals (Q) specimens. In all cases, however, the yield strength agreed well with that for the single crystal. The major trend consisted of a reduction of the easy glide region as the number of boundaries of the incompatible multi-crystals was increased. (The deviations of the stress-strain curves for the compatible multi-crystals from that for the single crystal might have arisen from small deviations from the ideal orientations or from grip effects.)

Elbaum also made detailed observations on the operative slip mechanisms. These are best described in the terminology of Rossi and Mathewson[37]: the plane on which the resolved shear stress is greatest is designated the principal plane. If the principal plane is the $(11\bar{1})$, the $(1\bar{1}1)$, $(\bar{1}\bar{1}\bar{1})$ and the $(\bar{1}11)$ are respectively designated the conjugate, cross-slip and critical planes. (1) Compatible crystals exhibited slip lines almost exclusively on the principal planes. A few slip lines were occasionally observed on the critical plane. After several percent elongation pronounced kink bands and occasional cross-slip were observed. These types of markings, however, were no more pronounced in the vicinity of the boundary than elsewhere over the surface of each grain. (2) The incompatible bicrystals ex-

hibited strain markings of the principal slip plane over the entire grain and weaker traces of the critical plane. The critical plane traces were more prevalent in the immediate vicinity of the boundary. (3) In the center grain of incompatible tri- and quadru-crystals strong markings of both the principal and critical slip planes were obtained, coupled with minor markings arising from slip on the conjugate planes. Elbaum attributed the higher rates of strain hardening of the incompatible tri- and quadru-crystal to the formation of Lomer-Cottrell dislocations due to slip on the principal and conjugate planes. In contrast, the lesser rate of strain hardening of the incompatible bicrystals suggested that the jogs formed by intersection of dislocations on the principal and critical planes are less effective barriers to dislocations than Lomer-Cottrell blocks. For strains greater than several percent as many as five or six slip systems acted in the vicinity of the boundary of two adjacent grains in the incompatible tri- and quadru-crystals.

A number of significant deductions, pertinent to the behavior of polycrystalline aggregates, have resulted from experimental investigations on the plastic behavior of bicrystals and multicrystals having vertical grain boundaries coincident with the tensile axis: 1. The grain boundary per se offers no resistance to plastic deformation. Isoaxial bicrystals having compatible orientations have the same stress-strain curves as similarly oriented single crystals. 2. The yield strength of incompatible as well as compatible isoaxial bicrystals is identical with that for similarly oriented single crystals. Thus, the differences in orientation of each gram of incompatible isoaxial bicrystals does not increase the stress for initiation of plastic deformation. 3. Incompatible isoaxial bicrystals strain harden at a much higher rate than similarly oriented single crystals. The increase in the rate of strain hardening can be ascribed principally to the operation of multiple slip (at least four systems) in the vicinity of the grain boundary, a condition which is imposed by the necessity of satisfying the compatibility relationships in the grain boundary region. 4. Multiple slip is most prevalent in the immediate

vicinity of the grain boundary of bicrystals and multicrystals. Consequently, the rate of strain hardening increases as the grain size of multicrystals decreases. 5. Multiple slip occurs almost exclusively on the usual slip systems found operative in single crystals, but occasionally new slip systems become operative.

VI. FULLY-DEVELOPED PLASTICITY IN POLYCRYSTALLINE AGGREGATES

All attempts to predict the plastic behavior of polycrystalline aggregates from the known behavior of single crystals are based on the assumptions that deformation in the polycrystalline aggregates takes place exclusively by the same slip systems and the same dislocation mechanisms as those operative in single crystals. These assumptions, however, are not generally valid. They are obviously incorrect when grain-boundary shearing becomes prevalent. Furthermore, Livingston and Chalmers[32] have reported examples of Al bicrystals that exhibit minor amounts of slip on the $\{110\}$ planes whereas slowly deformed single crystals slip exclusively on the $\{111\}$ planes. In addition, Hartmann and Macherauch[38] have stated that about 40% of the observed slip lines in polycrystalline Al arise from non-octahedral slip systems. However, it is unusually difficult to identify, unambiguously, slip systems from surface traces when cross-slip is prevalent.

The deformation rate of single crystals of F. C. C. metals at low temperatures is controlled by the intersection mechanism over Stages I and II.[23, 39] Only over the higher ranges of stress in Stage III does the stress assisted thermal activation of cross-slip take place in single crystals. On the other hand the applied stress is usually sufficiently high in polycrystals, especially in those having high stacking fault energies, to induce cross-slip to occur in the vicinity of the yield strength. Any serious attempt to predict the plastic behavior of polycrystalline aggregates from single crystal slip must be based on appropriate single crystal data referring to the same mechanisms as are operative in the polycrystalline aggregate.

The earliest attempts to predict the plastic behavior of polycrystalline aggregates from single crystal data were based on the assumption of elastic rigidity insofar as the elastic strains were neglected and the total strains were assumed to be exclusively plastic. This assumption is approximated in real materials only when the plastic strains are more than an order of magnitude larger than the elastic strains. Consequently, the early theories, to be described in this section, are not appropriate for estimating the conditions at yielding of originally annealed metals. The more recent attempts to predict the stress-strain behavior of polycrystals considering elastic as well as plastic strains will be discussed in the next section.

When a polycrystalline aggregate is deformed the following conditions must be satisfied:

1. Continuity of strains must be preserved across the grain boundary as discussed in Section V of this report.

2. Equilibrium of stresses must be preserved across the grain boundaries. Therefore, detailed treatment of the problem becomes prohibitively difficult.

3. Polyslip must take place.

Von Mises[40] has shown that at least five independent slip systems must become operative in each grain of the polycrystalline aggregate in order to preserve continuity of strain. The strain tensor appropriate to each grain defines six components of the strain which are related only by the equation of constancy of volume giving five independent components of the strain. Since the components of the strain are related linearly to the shear displacements for slip, at least five independent slip systems must operate.

The pioneering attempts by Sachs,[41] Cox and Sopwith,[42] Kochendorfer,[43] Calnan and Clews[44] and Batdorf and Budiansky[45] to estimate the plastic stress-strain curve of a polycrystalline aggregate only partly

fulfilled the above conditions. Several years ago, however, Taylor[46] presented a more acceptable analysis which attempted to satisfy, at least nominally, all necessary conditions. More reeently Bishop and Hill[47] and Bishop[48] have presented additional justification of Taylor's approach.

Taylor avoided the detailed analyses that are entailed in the second condition of equilibrium of stress across each grain boundary by invoking the energy principle. The work done in tensile straining a polycrystalline aggregate an amount $d\varepsilon$ at a stress σ is equal to the work done by slip. Therefore,

$$\sigma\, d\varepsilon = \sum \tau_i\, d\gamma_i \tag{18}$$

where τ_i is the critical shear stress for slip and $d\gamma_i$ is the increment of shear strain due to slip on the i th system. Furthermore, Taylor assumed that work hardening was isotropic insofar as he assumed that the average critical resolved shear stress was the same not only for each slip system but also from grain to grain. Single crystal studies reveal that the critical shear stress for slip is only approximately the same for the various slip systems. When slip takes place on one system, the shear stress for slip increases on all systems. In fact, the critical shear stresses for slip on the latent systems in metals are usually slightly greater than those for the operative system. In some ceramic single crystals, the hardening of the latent systems appears to be substantially higher than the hardening on the operative system. This factor indeed contributes to the brittleness of some polycrystalline ceramic materials. The assumption of equal strain hardening of all slip systems in metals undertaking polyslip, however, is quite good. Therefore, $\tau_i \simeq \tau_c$, and

$$\frac{\sigma}{\tau_c} = \frac{\sum |d\gamma_i|}{d\varepsilon} = m \tag{19}$$

In order to provide continuity across the grain boundaries, Taylor assumed that each grain exhibited identical strains, the strains being equal to those for the entire tensile bar. This assumption has been verified experimentally from the macroscopic viewpoint for large strains inasmuch as each grain deforms approximately as the bar itself. But Boas and Hargreaves[49], Urie and Wain,[50] and also Deshpande[51] have demonstrated from surface strain measurements that the strains are not necessarily uniform over a grain.

The requirement for continuity demands that at least five slip systems must become operative and contribute to the $\sum |d\gamma_i|$: The operative slip systems were taken to be those for which the plastic strain energy was least and therefore $\sum |d\gamma_i|$ was a minimum. Such a minimum is achieved only when no more than five systems operate. By detailed numerical analyses, Taylor found that the average value of $\bar{m}$ for random orientations of face-centered cubic metals was 3.06. Consequently $\sigma = 3.06\ \tau_c$. The average value of τ_c over all grains was determined from a single crystal stress-strain curve, where it was assumed

$$\tau_c \equiv \tau_c\left\{\int \sum |d\gamma_i|\right\} \equiv \tau_c\left\{\bar{m} \int d\varepsilon\right\} \qquad (20)$$

This assumption will be shown to be invalid and should be replaced by an appropriate strain-hardening curve for a single crystal undergoing polyslip.

Predictions by Taylor of the stress-strain curve for polycrystalline Al from single crystal data was fair. But as will be described later, this agreement was, in part, the result of a rather fortuitous selection of an inaccurate single crystal stress-strain curve.

Taylor also predicted the kind of preferred orientation that can be expected from tensile straining an originally randomly oriented F. C. C. poly-

crystalline aggregate. Barrett and Levenson[52] however revealed that the predictions made by Taylor differ appreciably from the experimental facts. Thus, the question arises as to whether Taylor's theory, although mechanistically incompetent to describe the actual details of the operative slip systems, may nevertheless be acceptable for estimating the stress-strain curve for polycrystals. This question was answered by Bishop and Hill.

Bishop and Hill have shown that Taylor's criterion, namely that $\sum |d\gamma_i|$ is a minimum for the operative system, is justified. Let $d\gamma_i^*$ be any set of shear strain that are geometrically equivalent to the actual set $d\gamma_i$ insofar as they provide the same tensile strains. Hence, the virtual work for deformation is given by

$$\sigma d\varepsilon = \sum \tau_i \cdot d\gamma_i = \sum \tau_i^* d\gamma_i^* \tag{18}$$

where τ_i^* is the resolved shear stress for the equivalent set of slips. For the operative set $\tau_i = \tau_c$ but since the resolved shear stress on the equivalent set cannot exceed the critical resolved shear stress for slip, $\tau_c \geq \tau_i^*$. Consequently

$$\sigma d\varepsilon = \tau_c \sum |d\gamma_i| \leq \tau_c \sum |d\gamma_i^*|$$

and

$$\sum |d\gamma_i| \leq \sum |d\gamma_i^*| \tag{21}$$

Eqn. (21) asserts that the sum of the absolute values of the operative shear set of shear strains is never greater than the set of geometrically equivalent shear strains.

Bishop and Hill have also presented a more rigorous analysis of the

problem of predicting the plastic behavior of polycrystalline aggregates. They adequately take into consideration the conditions of equilibrium as the local stress varies from point to point. They also admit that the strains, too, are inhomogeneous not only from grain to grain but also over a single grain. Hence, they need not invoke Taylor's assumption that each grain deforms homogeneously with the same strains as the aggregate. And they finally prove that the expected stress-strain curve agrees with that obtained by applying Taylor's assumptions. Their technique however is not fully developed in such a way as to permit a determination of the actual preferred orientation that results upon deformation. Consequently, the effects of re-orientation of the grains on strain hardening is neglected. However, Bishop[53] has shown that the theory can be extrapolated so as to give information on possible deviations from the re-orientations suggested by Taylor in such a way as to provide better agreement with the experimental facts.

To arrive at their conclusions, Bishop and Hill invoked the principle of maximum plastic strain energy. This principle asserts that the work of straining resulting from the actual state of stress σ_{ij} is greater than or equal to the work done by any other state of stress σ_{ij}^* that does not violate the yield condition. Therefore,

$$(\sigma_{ij} - \sigma_{ij}^*)\, d\varepsilon_{ij} \geq 0 \qquad (22)$$

for each small volume element.

To prove this condition, they employed the difference in work expression

$$dW - dW^* = (\sigma_{ij} - \sigma_{ij}^*)\, d\varepsilon_{ij} = \sum (\tau_i - \tau_i^*)\, d\gamma_i$$

where the term on the right hand side is determined from the slip in each part of a grain. But the last term is always positive, since $\tau_i = \tau_c$

and $\tau_i^* \leq \tau_c$; consequently, the condition given by Eqn. (22) is valid for all microscopic regions of the aggregate.

Let E_{ij} be the average strain in the aggregate, where

$$\varepsilon_{ij} = E_{ij} + \Delta\varepsilon_{ij} \tag{23}$$

The average value of $\int \Delta\varepsilon_{ij}\, dv = 0$ over a sufficiently large representation volume, v. Then

$$\int (\sigma_{ij} - \sigma_{ij}^*)\, d\varepsilon_{ij}\, dv =$$

$$\int \sigma_{ij}\, d\varepsilon_{ij}\, dv - \int \sigma_{ij}^*\, d\varepsilon_{ij}\, dv - \int \sigma_{ij}^*\, d\Delta\varepsilon_{ij}\, dv \geq 0 \tag{24}$$

It is permissible to associate the stress σ_{ij}^* with that which would have been obtained when the strain is E_{ij} since this stress cannot exceed the yield conditions. Then $\int \sigma_{ij}^*\, d\Delta\varepsilon_{ij}\, dv = 0$ since $\Delta\varepsilon_{ij}$ is in no way statistically related to σ_{ij}^*. When the integration is conducted over a representative unit cube

$$S_{ij}\, dE_{ij} - S_{ij}^*\, dE_{ij} \geq 0 \tag{25}$$

where S_{ij} is the actual average stress acting on a unit cube having the average increment of strain dE_{ij} and S_{ij}^* is the average stress when all grains undergo the average increment of strain; thus S_{ij}^* is the stress calculated by Taylor.

But when the local strain is dE_{ij} the operative stress

is σ^*_{ij} . Therefore, by analogy to Eqn. (22),

$$(\sigma^*_{ij} - \sigma_{ij})\, dE_{ij} \geq 0 \tag{26}$$

where σ_{ij} can now be associated with the actual local stress which of course cannot exceed the yield condition. Then

$$\int (\sigma^*_{ij} - \sigma_{ij})\, dE_{ij}\, d\nu = \int \sigma^*_{ij}\, dE_{ij}\, d\nu - \int \sigma_{ij}\, dE_{ij}\, d\nu + \int \sigma_{ij}\, d\Delta E_{ij}\, d\nu \geq 0 \tag{27}$$

But inasmuch as σ_{ij} and $\Delta \varepsilon_{ij}$ are not statistically related the last integral is zero, and

$$S^*_{ij}\, dE_{ij} - S_{ij}\, dE_{ij} \geq 0 \tag{28}$$

Comparing Eqns. (25) and (28) reveals that

$$S_{ij} = S^*_{ij} \tag{29}$$

namely that Taylor's theory indeed gives the correct stress in spite of the fact that the local stresses, strains and re-orientation of the grains deviate from those suggested by his assumptions.

Bishop and Hill calculated the yield strength of a randomly oriented polycrystalline aggregate. They define the average value of the critical resolved shear stress $\bar{\tau}$ over the aggregate as

$$\bar{\tau} = \int \tau\, d\nu$$

where τ is the value in any individual grain taken to have the same

value regardless of sign. Thus, the Bauschinger effect is neglected. If σ_{ij}^* produces a strain dE_{ij} in a grain in which the critical resolved shear stress is τ, the average stress $\bar{\sigma}_{ij}^* = \bar{\tau}\sigma_{ij}/\tau$ would produce the same strain in a grain of the same orientation having the average critical resolved shear stress. Then

$$\int \bar{\tau}\sigma_{ij}\,dv = \int \tau\,\bar{\sigma}_{ij}^*\,dv = \bar{\tau}\int \bar{\sigma}_{ij}^*\,dv \qquad (30)$$

when it is observed that there is no statistical correlation between τ and $\bar{\sigma}_{ij}^*$. Therefore

$$\int \sigma_{ij}\,dv = \int \bar{\sigma}_{ij}^*\,dv = S_{ij}^* = S_{ij} \qquad (31)$$

and consequently the strain energy can be calculated using the average critical resolved shear stress in the aggregate.

To determine the yield condition for a randomly oriented polycrystalline aggregate of a face-centered cubic metal, Bishop and Hill invoked the principle of maximum plastic strain energy in preference to Taylor's selection of the minimum sum $(\sum |d\gamma_i|$ of the absolute values of the shear strains in slip. They demanded that the average critical resolved shear stress be reached on sets of five slip systems each, and calculated therefrom the corresponding sets of $\bar{\sigma}_{ij}^*$. When those sets for which the shear stress on other slip planes exceeded $\bar{\tau}_c$ were discarded as violating the yield condition, only fifty-six sets of physically possible stresses $\bar{\sigma}_{ij}^*$ remained. To each set of stresses there exists a corresponding set of shear strains. But it is not necessary to consider these in detail. Assuming an average imposed increment of strain dE_{ij} that set of stresses which provides the greatest work can, by the application

of the principle of maximum plastic strain energy, be identified as the operative set. When $dW\{\varphi, \theta, \psi$ is the increment of maximum work for the imposed strain referred to the Eulerian angles, φ . θ . ψ ,

$$S_{ij}\, dE_{ij} = \frac{\int\int\int dW \sin\theta \, d\varphi \, d\theta \, d\psi}{\int\int\int \sin\varphi \, d\varphi \, d\theta \, d\psi}$$

By this technique Bishop and Hill also find that S = 3.06 τ_c for simple tension. Furthermore, Bishop and Hill demonstrated that the plastic potential calculated on the basis of their theory lies between the Tresea and von Mises criteria for yielding under combined stresses, a deduction which is in good agreement with the best current experimental evidence.

We have already noted in Section IV that single crystals do not have a unique stress-strain curve, the rate of strain hardening being dependent on the initial orientation. The differences in strain hardening arise from the fact that those orientations which are more favorable for the operation of secondary slip systems give the higher rates even when the total amount of slip on such systems may be rather negligible. Thus, the question arises as to what single crystal stress-strain curve might be used to predict the behavior of a polycrystalline aggregate. Kocks[54] pointed out that inasmuch as slip must take place on at least five slip systems, the appropriate data for predicting the polycrystalline stress-strain curve must be obtained from single crystals that are so oriented that slip can take place simultaneously on many slip systems. There are two orientations in F.C.C. metals that provide simultaneous polyslip on more than two slip systems: crystals oriented so that the tensile axis is aligned along the [100] direction slip simultaneously on eight systems and crystals oriented so that the tensile axis

is aligned along the [111] direction slip on six systems. Howe and Elbaum[55] have shown, however, that the [100] orientation does not give stable polyslip since small deviations from this orientation lead to the operation of only two slip systems. Consequently, the most appropriate single crystal polyslip data for predictions are obtainable only from orientations where the tensile axis is in the [111] direction. Although each operative system undertakes the same strain, the assumption that $\tau_i = \tau_c$ for all systems is not necessarily valid and will require detailed study in terms of dislocation interactions. Furthermore, it is not immediately apparent that the same values of τ_c as a function of γ will be obtained for the six operative systems as might result from the operation of only five systems in the polycrystalline aggregate.

For calculating the stress-strain curve of a polycrystalline aggregate Kocks used a simple analysis that is the substantial equivalent of Taylor's method and is consistent with the deductions based on the work of Bishop and Hill. In each element of a grain

$$\sigma \cdot d\varepsilon = \sum \tau_i \, d\gamma_i = \tau_c \sum d\gamma_i \qquad (32)$$

where σ and ε are tensors and where the strain hardening in this element is assumed to be isotropic. The value of $\sum d\gamma_i$ is related linearly to the strain tensor by the tensor M, where

$$\sum d\gamma_i = M \cdot d\varepsilon \qquad (33)$$

and, therefore,

$$\sigma = \tau_c M \tag{34}$$

The tensor, M, is exclusively determined by the orientation of the slip planes and directions to the axes of the specimen. For a single crystal undergoing single slip, M is simply given by the Schmid factor

$$[\cos\lambda \cos(90-\chi)]^{-1}$$

The macroscopic work over a representative volume is

$$S_{ij}\, dE_{ij} = \overline{\sigma\, d\varepsilon} = \overline{\tau_c \sum d\gamma_i} = \bar{\tau}_c \overline{\sum d\gamma_i} \tag{35}$$

$$= \bar{\tau}_c \overline{\sum M\, d\varepsilon} = \bar{\tau}_c \bar{M}\, dE_{ij}$$

where the averaging is done over all microscopic volumes in a representative macroscopic unit volume. The second equality assumes τ_c has the same value for all slip systems in each microscopic volume and the third equality is based on the fact that the local resolved shear stress is unrelated to the increment of shear strains. The fourth equality arises from Eqn. (33) and the fifth is valid because $d\varepsilon$ is not statistically related to M. Therefore, in a tension test

$$S = \bar{\tau}_c \bar{M} \tag{36}$$

The critical shear stress in each microscopic volume is assumed to be given by

$$\tau_c \equiv H\{\int \sum d\gamma_i\} \equiv H\{\int M \cdot d\varepsilon$$

and therefore

$$\bar{\tau}_c \equiv H\{\overline{\int M d\varepsilon}\} = H\{\bar{M}E\} \qquad (37)$$

where $E = \int d\varepsilon$ and the validity of the second equality arises from the fact that $d\varepsilon$ is statistically unrelated to M. As shown by Taylor, $\bar{M} \simeq 3.06$. The agreement obtained between the calculated stress-strain curve based on the single crystal data where the tensile axis is in the $[111]$ direction and that of a polycrystalline aggregate of Al is shown in Fig. 21. The agreement is exceptionally good for large strains.

It is well-established that the flow stress of polycrystalline aggregates decreases as the grain size increases. A typical example of this effect is shown in Fig. 22 for Al,[56] and in Fig. 23 for Cu alloys[57] as presented by Zener.[58] Although no exceptions to these trends have been reported, none of the theories so far considered in this report have been so formulated as to take into account the grain size effects. Obviously, the nominal agreement that has been noted between a prediction of the stress-strain curve of polycrystalline aggregate based on theory with that obtained experimentally for one grain size must be somewhat accidental.

It is possible, of course, that some of the observed decrease in flow strength with increasing grain size arises not from a grain size effect per se but rather as a result of modification of the substructure of the grains. For, when a metal is annealed for a longer time or at a higher temperature in an attempt to coarsen the grain size, the pattern of dislocations can well change as a result of cross-slip or climb to provide a more dislocation free and, therefore, softer metal. Undoubtedly, some effects attributed to grain size are due to this factor and others may be associated with effects of small amounts of impurities. On the other hand, the rather consistent

relationship between the flow stress and the reciprocal of the square root of the grain diameter, as shown in Fig. 23, for a number of cases would not necessarily be obtained if the effects were solely due to difference in dislocation densities. Furthermore, as shown in Fig. 22 the major effect of grain size appears to involve a greater rate of strain hardening for the finer grain sizes, whereas the expected trend for a greater density of dislocations is a lower rate of strain hardening, as is commonly observed during deformation in a single stress-strain curve. We are, therefore, led to believe that a true grain size effect exists although in any real example it can be accompanied by other effects as well.

Dislocation theory suggests that the true grain size effect arises from the stress fields due to dislocations that are piled-up against barriers. Local stresses due to such arrays can be several orders of magnitude greater than the applied stress and consequently these stress fields frequently assume significant importance. Koehler[59] first studied this phenomenon which was subsequently treated in a more general way by Eshelby, Frank and Nabarro.[60] The number of dislocations that can be packed into an arrested array is given by

$$n = \alpha \pi \frac{(\tau - \tau_G) L}{Gb} \qquad (38)$$

where τ is the applied shear stress on the slip plane, τ_G is the stress representing the resistance to the motion of a dislocation, L is the piled up distance which is approximately equal to $D/2$ when the grain boundary of a grain having a diameter D is the barrier, G is the shear modulus of elasticity and b is the Burger's vector. Stroh[61] has shown that the local shear stress at a distance l from the barrier is approximately

$$\tau_l = (\tau - \tau_G)\sqrt{\frac{D}{l}}$$

If slip is to be propagated to the adjacent grain, a sufficient number of mechanisms of slip must be stimulated so that the deformation on a microscopic scale satisfies the detailed boundary conditions for slip. This requirement is much more severe than the macroscopic requirement of continuity. Consequently, the local stress that must be achieved to satisfy this condition is greater than the value of τ_c for polyslip so adjusted only to satisfy the macroscopic conditions of continuity. Therefore, the applied shear stress for slip is given by

$$\tau - \tau_G = \tau_\ell \sqrt{\frac{\ell}{D}} \tag{39}$$

where τ_ℓ is now the local value of the shear stress required to initiate sufficient number of slip mechanisms to satisfy the stringent conditions of microscopic continuity. Thus, the applied shear stress increases as the reciprocal of the square root of the grain diameter. Unfortunately the necessary detailed statistical analyses that are suggested by this approach have not yet been made.

VII. INITIAL STAGES OF PLASTIC DEFORMATION

In their approach to the problem of the plastic behavior of polycrystalline aggregates Taylor and also Bishop and Hill, as presented in Section VI, assumed that the strains were exclusively plastic. Whereas this assumption is reasonably valid for large strains, particularly where the stress-strain curve is not too steep, the assumption is invalid in real polycrystalline aggregates in the small strain region. Here it is necessary to consider the elasto-plastic straining since the plastic strains are the same order of magnitude as the elastic strains. Because of the theoretical significance as well as the practical importance of plastic yielding, the problem of the initial stages of plastic deformation is one of paramount interest in

solid state mechanics.

Damping capacity investigations clearly reveal that plastic deformation begins to take place at very low stress levels, much below the so-called conventional proportional limit. Due to the effects of the heterogeneity of dislocation patterns and the effects of orientation of grains on their flow strength, slip first occurs statistically in relatively few so-called "soft grains" of the aggregate. The extent of this slip in any one grain is limited by the surrounding elastic matrix. When the stress is removed, back stresses, arising from the elastic strains in the matrix, force the dislocations to return to their origin, the aggregate having the properties of an anelastic solid. As the stress is increased the "softest grains" undertake larger strains, and under usual circumstances undergo polyslip, and other grains also begin to slip. Under polyslip, barriers may be formed that prevent the complete back motion of the dislocations upon removal of the stress and small permanent strains are obtained. At sufficiently high stresses, of course, all of the grains are subjected to plastic deformations and only a small part of the total strain is recoverable.

A zeroth order analysis of the microstrain behavior of polycrystalline aggregates was suggested by Thomas and Averbach[62] and subsequently elaborated by Brown and Lukens.[63] Their statistical analysis obviously requires major improvement but their concepts are presented here primarily to illustrate the possible role of grain size on the plastic behavior of polycrystals in the small strain region.

The assumption was made that when a stress that is sufficiently high to stimulate a Frank-Read source is applied to a polycrystal a number of dislocations sweep across the entire grain area and become arrested at the boundary. The plastic shear strain in the i th grain is then approximated by

$$\gamma_i^p = m_i D^2 b \rho \qquad (40)$$

where m_i is the number of dislocations in the piled up array, D^2 (the square of the grain diameter) is approximately the area swept out per dislocation, b is the Burger's vector, and ρ is the density of sources, which is assumed to be uniform throughout the polycrystalline aggregate. The gross assumption is now made that the contribution of this local plastic strain to the total strain over the entire specimen is proportional to the fraction of the volume occupied by the grain, namely about D^3/Al where A is the cross-sectional area and l is the specimen length. Consequently, the contribution of slip in the i th grain to the observed total plastic strain is taken to be about

$$\gamma_i^{\rho} = m_i D^2 b \rho D^3/Al \tag{41}$$

The number of dislocation loops per source at the boundary is given by the well-known expression of Eqn. (38)

$$m_i = (\sigma - \sigma_{oi}) \frac{2D}{Gb} \tag{42}$$

where σ is the applied shear stress, σ_{oi} is the local stress necessary to activate a Frank-Read source in the i th grain, and G is the shear modulus of elasticity. Each grain is assumed to exhibit different values of σ_{oi} the fraction of the grains that have values in the range $d\sigma_{oi}$ being $f_i\, d\sigma_{oi}$. Consequently, the number of grains in the specimen that have values of σ_{oi} in the range $d\sigma_{oi}$ are

$$f_i \frac{Al}{D^3} d\sigma_{oi}$$

Then

$$\gamma = \int_i \gamma_i f_i \frac{Al}{D^3} d\sigma_{oi} \tag{43}$$

The distribution function $f_i\, d\sigma_{oi}$ was assumed to be approximately that suggested by the Schmid factor for randomly oriented grains. Thus, the effects of statistical distribution of sizes of Frank-Read sources was neglected. Brown and Lukens estimate that the plastic strain is, therefore, given by

$$P_\gamma = \frac{\rho D^3 (\sigma - \sigma_o)^2}{2G\sigma_o} \qquad (44)$$

In spite of the rather crude statistical approach that was adopted, Eqn. (44) nevertheless represents the experimental trends quite well. It predicts the following: 1) The stress at which plastic straining first begins is independent of the grain size, 2) The stress increases as the square root of the plastic strain, and 3) The plastic strain increases with the cube of the grain diameter.

A typical result is shown in Fig. 24 confirming the nominal validity of Eqn. (44). The value of the calculated density of sources, however, appears to be slightly too high.

A more sophisticated approach to the early plastic behavior of polycrystalline aggregates was recently presented by Budiansky, Hashin and Sanders.[64] Their analyses consist of extensions of Eshelby's[65] determination of the stress field produced when a grain in an elastic matrix undertakes homogeneous strains. Eshelby has shown that when an ellipsoidal inclusion strains homogeneously an amount $^{T}\varepsilon_{kl}$ in the absence of constraints, the strains $^{c}\varepsilon_{ij}$ it experiences under constraint in an elastic matrix are also homogeneous, being given by

$$^{c}\varepsilon_{ij} = S_{ijkl}\, ^{T}\varepsilon_{kl} \qquad (45)$$

where S_{ijkl} are constants that can be evaluated in terms of integral

elliptic functions.

The assumption is made that slip can be treated as a homogeneous deformation. The value of $^{T}\varepsilon_{kl}$ for slip, however, is not prescribed geometrically as it is in the simpler cases of twinning and phase transformations. Rather, it is limited by the constraints imposed by the surrounding elastic matrix. Under any condition, however,

$$^{T}\varepsilon_{kl} = \varepsilon_{kl} - L(\sigma_{kl}) \tag{46}$$

where ε_{kl} and σ_{kl} are the total strains and stresses in the inclusion and where $L(\sigma_{kl})$ represents the elastic strains as given by the stresses in terms of Hookes Law. Slip occurs when the entire aggregate is subjected to a critical stress σ_{ij}^{o} at infinity. The strains in the inclusion are, therefore, due to the superposition of the strains due to elastic deformation as a result of the loading and those arising from slip. Consequently

$$\varepsilon_{ij} = L(\sigma_{ij}^{o}) + S_{ijkl}\,{}^{T}\varepsilon_{kl} \tag{47}$$

The unknown values of $^{T}\varepsilon_{kl}$, ε_{ij} and σ_{ij} must be then found in terms of σ_{ij}^{o} by simultaneous solution of Eqns. (2)and (3) together with the stress-strain relationship for slip in the elasto-plastic inclusion.

When the grain undergoing homogeneous straining as a result of slip is spherical, S_{ijkl}, as shown by Eshelby, assumes the simple values such that

$$ {}^{c}e = a^{T}e = \frac{1}{3}\,\frac{(1+\nu)}{(1-\nu)}\,{}^{T}e \qquad (48) $$

and

$$ {}^{c}e_{ij} = b^{T}e_{ij} = \frac{2}{15}\,\frac{(4-5\nu)}{(1-\nu)}\,{}^{T}e_{ij} \qquad (49) $$

where ν is Poisson's ratio (isotropic elasticity being assumed, the elastic constants being the same in the inclusion as in the matrix) $e = \varepsilon_{ij}$ (where the usual tensor summation rule applies and therefore e is the volumetric strain),

$$ e_{ij} = \varepsilon_{ij} - \frac{1}{3}\,\delta_{ij}\,e $$

(the deviatoric strains) and δ_{ij} is the Kronecker delta.

The ratios of the components of the stresses σ^{o}_{ij} are assumed to be held constant during monotonic loading. For small stresses every grain of the polycrystalline aggregate strains elastically and homogeneously. When some critical value of σ^{o}_{ij} is reached some grains begin to yield plastically by slip. At yet higher stresses these grains exhibit more extensive slip and others begin to slip. One or several slip systems may operate in each slipping grain.

Let the operative slip system in a single grain be designated by the unit vectors $m_i^{(q)}$ normal to the slip plane and $n_i^{(q)}$ in the slip direction, where q denotes a given slip system. When only the first slip system is operative the plastic strain is given by

$$ {}^{p}\varepsilon_{ij} = \gamma_i\, a'_{ij} \qquad (50) $$

where γ_i is the engineering shear strain referred to the first slip

system and

$$a'_{ij} = \frac{1}{2}\left(m_i' n_j' + m_j' n_i'\right) \tag{51}$$

The plastic strain given by Eqn. (7) is Eshelby's unconstrained strain, and therefore

$$^{P}\varepsilon_{ij} = {}^{P}e_{ij} = {}^{T}\varepsilon_{ij} = {}^{T}e_{ij} \tag{52}$$

the mean volumetric strain being zero for slip. Consequently, introducing Eqns. (50) and (49) into Eqn. (47), the total strain in the grain is

$$\varepsilon_{ij} = L\left(\sigma^{\circ}_{ij}\right) + b\,\gamma_1\, a'_{ij} \tag{53}$$

The elastic strain in the grain is given by

$$^{E}\varepsilon_{ij} = L\left(\sigma^{\circ}_{ij}\right) + (b-1)\,\gamma_1\, a'_{ij} \tag{54}$$

as shown by subtracting the plastic strain Eqn. (50) from the total strain Eqn. (53). And, therefore, applying Hooke's law to Eqn. (54) the stress in the grain is

$$\sigma_{ij} = \sigma^{\circ}_{ij} - 2G(1-b)\,\gamma_1\, a'_{ij} \tag{55}$$

where G is the shear modulus of elasticity.

Although the concept of strain hardening could have been incorporated into the analysis, Budiansky et al, assumed zero strain hardening in order to simplify the analysis. On this basis, where τ_y is the constant

resolved shear stress for slip

$$\tau_y = \sigma_{ij}\, a'_{ij} \tag{56}$$

Multiplying Eqn. (55) by a_{ij} reveals that

$$\tau_y = \tau_1^{\circ} - G(1-b)\,\gamma_1 \tag{57}$$

where τ_1° is the applied shear stress on the slip plane due to the external loading and where $a'_{ij} \cdot a_{ij}$ is given its value of 1/2. Eqn. (57) then identifies the magnitude of γ_1 in terms of the externally applied shear stress on the slip plane, τ_1°, and the yield strength, τ_y. Introducing this value of γ_1 into Eqn. (55) gives the useful result

$$\sigma_{ij} = \sigma_{ij}^{\circ} - 2(\tau_1^{\circ} - \tau_y)\, a'_{ij} \tag{58}$$

and, by Eqn. (50), the complementary expression

$$^{P}\varepsilon_{ij} = \gamma_1 a'_{ij} = \frac{\tau_1^{\circ} - \tau_y}{G(1-b)}\, a'_{ij} \tag{59}$$

is also obtained.

The stress-strain relationship for a heterogeneous polycrystalline aggregate can be related to the strain energy of the system. For a monotonically increasing stress, the increase in strain energy per unit volume under simple tension is always

$$dw = \sigma\, d\varepsilon$$

regardless of the constitutive relations. Consequently, the tensile atrain

is

$$\varepsilon = \int_0^{\sigma} \frac{d\omega}{d\sigma} \frac{d\sigma}{\sigma} \tag{60}$$

A strain energy function also exists, for monotonically increasing proportional loading under combined stresses. Here

$$\varepsilon_{ij} = \int_0' \frac{\partial \omega \{\lambda \sigma_{ij}^{\circ}\}}{\partial \sigma_{ij}} \frac{d\lambda}{\lambda} \tag{61}$$

where ω is given as a function of $\lambda \sigma_{ij}^{\circ}$. The plastic strain of the entire aggregate is therefore given by

$$^{p}\bar{\varepsilon}_{ij} = \int_0' \frac{\partial\, ^{p}\omega}{\partial \sigma_{ij}} \frac{d\lambda}{\lambda} \tag{62}$$

where $^{p}\omega$ is the extra energy per unit total volume expressed in terms of $\lambda \sigma_{ij}^{\circ}$ arising from slip in some of the grains.

The plastic strain energy must be evaluated in terms of the external loading. Consequently, the work done per unit volume of a slipping grain is given by

$$^{p}\omega_r = \int_0^{^{p}\varepsilon_{ij}} \sigma_{ij}^{\circ}\, d\,^{p}\varepsilon_{ij} \tag{63}$$

As indicated by Eqn. (57)

$$\tau_r^{\circ} = \sigma_{ij}^{\circ}\, a_{ij}^{r} \tag{64}$$

and, from Eqn. (59) identifying the index 1 with r

$$d^{p}\varepsilon_{ij} = \frac{a_{ij}^{r}\, d\tau_r^{\circ}}{G(1-b)}$$

Therefore

$$^{p}w_r = \int_{\tau_y}^{\tau_r^{\circ}} \frac{\tau_r^{\circ}\, d\tau_r^{\circ}}{G(1-b)} \tag{65}$$

The plastic strain energy per unit volume of the aggregate is then

$$^{p}w = \frac{1}{V}\sum V_r\, ^{p}w_r \tag{66}$$

where V_r/V is the fraction of total volume occupied by grains of the r th kind and the summation is taken over the entire volume of slipping grains.

As seen by introducing Eqn. (66) into Eqn. (62)

$$^{p}\bar{\varepsilon}_{ij} = \int_0^{\lambda} \frac{1}{V}\sum V_r \frac{\partial\, ^{p}w_r}{\partial \sigma_{ij}^{\circ}} \frac{d\lambda}{\lambda} \tag{67}$$

$$\text{or}\quad ^{p}\bar{\varepsilon}_{ij} = \frac{\sum V_r}{V}\int_0^{\lambda} \frac{\partial\, ^{p}w_r}{\partial \sigma_{ij}^{\circ}} \frac{d\lambda}{\lambda}$$

But

$$\frac{\partial w_r(\lambda\sigma_{ij})}{\lambda\, \partial\sigma_{ij}^{\circ}} = \frac{\tau_r^{\circ} - \tau_y}{G(1-b)}\, a_{ij}^{r} \tag{68}$$

and

$$\int_0^{\lambda} \frac{\partial w_r}{\partial \sigma_{ij}} \frac{d\lambda}{\lambda} = \int_0^{\lambda} \frac{\lambda(\tau_r^{\circ} - \tau_y)}{G(1-b)}\, a_{ij}^{r} \frac{d\lambda}{\lambda} \tag{69}$$

$$= \frac{\tau_r^\circ - \tau_y}{G(1-b)} a_{ij}^r$$

Therefore,

$$\overline{{}^{p}\varepsilon_{ij}} = \sum \frac{V_i}{V} \frac{(\tau_r^\circ - \tau_y) a_{ij}^r}{G(1-b)} \tag{70}$$

for $\tau_r^\circ \geq \tau_y$ and $\overline{{}^{p}\varepsilon_{ij}} = 0$ when $\tau_r^\circ \leq \tau_y$

In order to evaluate Eqn. (70), the summation over all orientations was represented in terms of the integral over the Eulerian angles so that

$$\overline{{}^{p}\varepsilon_{ij}} = \frac{\iiint \sin\varphi \frac{(\tau_r^\circ - \tau_y) a_{ij}^r}{G(1-b)} d\varphi d\theta d\psi}{\iiint \sin\varphi \, d\varphi d\theta d\psi} \tag{71}$$

τ_i° was expressed in terms of the applied stress and the appropriate direction cosines for slip on the first active system. The term a_{ij}^r was also expressed in terms of direction cosines referred to the stereographic projection.

The final results are given in Fig. 25 in terms of the dimensionless ratios σ/σ_y and $\varepsilon/\varepsilon_y$ where σ_y and ε_y refer to the stress and the strain at which the grains first begin to slip. The data for slip on one system represents an upper bound to the expected results because several slip systems must operate at the higher stresses and because work hardening was neglected. Multiple slip was also considered by Budiansky, et al.

Undoubtedly, the most serious criticism of this approach results from the fact that the interactions between adjacent slipped grains was neglected. Consequently, the predicted stress-strain curve does not reveal the rather well-established dependency on grain size. Furthermore, the stress concentrations due to piled-up arrays of dislocations will cause adjacent grains to undergo slip earlier than the theory estimates they will. To a first approximation σ/σ_y should become asymptotic to Taylor's approximation at high strains. But Taylor's approximation is exceeded by the theory. A better asymptotic value is obtained assuming polyslip but the major difficulty appears to center around the neglect of interaction effects between slipped grains as the concentration of slipped grains becomes large.

VIII. KRONER'S THEORY

Recently, Kroner[66] developed a new analytical procedure for predicting the stress-strain behavior of polycrystalline aggregates when an "effective" single crystal stress-strain curve is known. It conveniently includes consideration of the elastic and plastic strains over all ranges of plastic strains. Furthermore, it is so formulated that the essential features of the Bauschinger effect, which was neglected in Bishop and Hill's as well as Taylor's methods, is automatically incorporated into the theoretical structure. Whereas Bishop and Hill and also Taylor adopted the average macroscopic strain as the appropriate independent variable, Kroner uses the new concept of employing the local "effective" stress for this purpose. Since the plastic behavior of a grain depends directly on this stress, Kroner's method obviates the need for applying such special selection principles for identifying the operative slip mechanism as Taylor's criterion of $\sum |d\varepsilon_i|$ is a minimum or Bishop and Hill's criterion of greatest plastic strain energy. Inasmuch as the local "effective" stress determines the operative slip systems,

we believe that predictions of changes in preferred orientations with straining based on appropriate extensions of Kroner's method of analysis to this problem should be in better agreement with the experimental facts than those based on Taylor's or Bishop's methods. But inasmuch as Kroner employs only the average stress on all grains having the same orientation, his approach neglects the effects of heterogeneous deformation over a single grain. Consequently, his technique cannot be expected to give the correct preferred orientations due to deformation.

Kroner identifies the orientation of each grain with respect to the axes of the aggregate in terms of the Eulerian angles φ , θ and ψ . Consequently, the frequency of any orientation in a randomly oriented polycrystalline aggregate is given by

$$\frac{d\Omega}{\Omega} = \frac{\sin\varphi\, d\varphi\, d\theta\, d\psi}{8\pi^2} \tag{72}$$

The average stress and plastic strain in any grain of the group having orientations between Ω and $\Omega + d\Omega$ are designated by σ_Ω and ε_Ω , respectively, where

$$\varepsilon_\Omega = f_\Omega \{\sigma_\Omega\} \tag{73}$$

is the effective stress-plastic strain relationship for a single crystal of orientation Ω . The average stress of the group of grains Ω can be related to the average macroscopic stress, $\bar{\sigma}$, applied to the entire aggregate by

$$\sigma_\Omega = \bar{\sigma} + \sigma_\Omega^E \tag{74}$$

where σ_Ω^E is a characteristic average stress of the group. We demonstrate later that

$$\sigma_\Omega \equiv \sigma_\Omega [\bar{\sigma}] \tag{75}$$

Then, the average macroscopic plastic strain $\bar{\varepsilon}$ in the aggregate can be represented by

$$\bar{\varepsilon} = \frac{1}{8\pi^2}\int \varepsilon_\Omega \, d\Omega = \frac{1}{8\pi^2}\int f_\Omega\{\sigma_\Omega\}\, d\Omega$$

$$= \frac{1}{8\pi^2}\int f_\Omega\{\sigma_\Omega[\bar{\sigma}]\}\, d\Omega \equiv F\{\bar{\sigma}\} \qquad (76)$$

The essential features of Kroner's theory are given by Eqn. (76). When the effective stress σ_Ω is established as a function of the average applied stress $\bar{\sigma}$ and when the effective stress σ_Ω is known as a function of the plastic strain ε_Ω, as deduced from appropriate single crystal tests, the macroscopic strain, $\bar{\varepsilon}$, is calculable in terms of the macroscopic stress, $\bar{\sigma}$.

To deduce the required relationship between the effective stress and the macroscopic stress $\bar{\sigma}$, it is necessary to analyze the sources of the characteristic stress σ_Ω^E defined by Eqn. (74). The total characteristic stress can be visualized as arising from two effects so that

$$\sigma_\Omega^E = \sigma_\Omega^{E'} + \sigma_\Omega^{E''} \qquad (77)$$

For example, as $\bar{\sigma}$ is increased those grains most favorably oriented for slip will be the first to undertake plastic deformation. The stress on this group will correspondingly deviate from the average stress $\bar{\sigma}$ by an amount dictated by the back stress, σ_Ω^E, due to constraint offered by the surrounding elastic matrix. As each grain of the group slips, however, a higher stress is imposed on the remaining grains of the group. This stress will have the average value of $\sigma_\Omega^{E''}$ for the group taken as a unit. But the two characteristic stresses are not

independent since their average over a representative cross-section must equal zero. Therefore,

$$\sigma_\Omega^{E'} \frac{d\Omega}{8\pi^2} + \sigma_\Omega^{E''} = 0 \tag{78}$$

a As the macroscopic stress is further increased other groups will begin to deform and thus contribute to $\sigma_\Omega^{E''}$ so that

$$\sigma_\Omega^{E} = \sigma_\Omega^{E'} + \sum_\Omega \sigma_\Omega^{E''} \tag{79}$$

On introducing Eqn. (78) into Eqn. (79)

$$\sigma_\Omega^{E} = \sigma_\Omega^{E'} - \frac{1}{8\pi^2} \int \sigma_\Omega^{E'} d\Omega \tag{80}$$

In passing we wish to point out that the major criticism that can be leveled against the Budiansky, Hashin and Sanders method centers about their neglect of this interaction effect.

Although in principle an exact solution is obtainable, it was desirable in order to facilitate the calculation to make the following assumptions:

1. The volume remains constant during plastic deformation.
2. The elastic anisotropy of the grains is neglected.
3. The linear theory of elasticity is assumed valid.

Accordingly, the plastic strain ε_Ω is a deviator and consequently the stresses arising from it are deviatoric. Applying Eshelby's relationship for constrained deformation

$$\sigma_\Omega^{E'} = -\alpha G \varepsilon_\Omega \tag{81}$$

where G is the shear modulus of elasticity and α = 16/15 for a spherical

grain. Therefore, from Eqns. (74), (80), and (81)

$$\bar{\sigma} = \sigma_\Omega + \alpha G\left[f_\Omega\{\sigma_\Omega\} - \frac{1}{8\pi^2}\int f_\Omega\{\sigma_\Omega\}\,d\Omega\right] \quad (82)$$

Therefore, given the appropriate single crystal stress-strain curves, $f_\Omega\{\sigma_\Omega\}$, it is possible to calculate $\sigma_\Omega\{\bar{\sigma}\}$ which can then be introduced into Eqn. (76) to obtain the plastic strain $\bar{\varepsilon}$ as a function of the applied stress $\bar{\sigma}$ for the aggregate.

The major difficulty in applying Kroner's theory concerns the possibility of obtaining appropriate single crystal stress-strain curves. Obviously, the plastic behavior of a grain in a polycrystalline aggregate differs in several significant ways from the behavior of a single crystal:

1. During Stage I of a single crystal test the dislocations can leave the crystal whereas in a grain of a polycrystalline aggregate such dislocations may pile up at the grain boundary. Such pile-ups will be relaxed by cross-slip and slip on secondary systems, thereby introducing barriers and increased density of the forest dislocations.

2. Whereas Kroner has introduced an orientation factor, we recognize that this is not the only appropriate independent variable; rather the effect of orientation depends on the nature of the dislocation reactions that result. Such dislocation reactions are decidedly different under the conditions of polyslip that actually occurs in the polycrystalline aggregate.

3. As in the case of other theories for the plastic deformation of polycrystalline aggregates, Kroner's theory does not contain any reference to the well-documented effect of grain size increasing the rate of strain hardening. This factor must also be introduced in the $f_\Omega(\sigma_\Omega)$ curves.

It appears to the present authors that it will be very difficult to obtain desired appropriate individual grain $f_\Omega(\sigma_\Omega)$ curves from single crystal data. It may be possible, in terms of a deeper knowledge of the dis-

location theory for strain hardening; however, to calculate from theoretical considerations the appropriate curve. This attempt is justified in terms of the rather excellent and complete theoretical basis of the Kroner theory.

ACKNOWLEDGMENT

The authors wish to acknowledge that this paper was written in cooperation with the Lawrence Radiation Laboratory under sponsorship of the United States Atomic Energy Commission. John E. Dorn also wishes to thank Dr. H. Thiemann, Director of Battelle Memorial Institute at Geneva, for the opportunity of preparing the major portion of this manuscript while he was a guest at the Battelle Laboratories in Geneva in the late Fall of 1961.

REFERENCES

1. L. M Clarebrough and M. E. Hargreaves, "Work Hardening of Metals", Prog. Metal Physics, 8 (1959) Chapter 1.

2. A. Seeger, "The Mechanism of Glide and Work Hardening in Face-Centered Cubic and Hexagonal Close-Packed Metals", Dislocations and Mechanical Properties of Crystals, John Wiley and Sons, New York (1957)pp. 243-329.

3. J. Friedel, "Dislocation Interactions and Internal Strains", Internal Stresses and Fatigue in Metals, Elsevier Publishing Company (1959) pp. 220-262.

4. G. Schoeck, "Thermodynamic Principles in High-Temperature Materials", Mechanical Behavior of Materials at Elevated Temperatures, McGraw-Hill Book Company, Inc., New York (1961) Chapter 5.

5. F. E. Hauser, P. R. Landon, and J. E. Dorn, "Deformation and Fracture Mechanisms of Polycrystalline Magnesium at Low Temperatures", Trans. ASM, 48 (1956) pp. 986-1002.

6. E. O. Hall, "Twinning and Diffusionless Transformations in Metals", Butterworth and Co., Ltd., London (1954)

7. W. Boas and E. Schmid, "Uber die Temperaturabhangigkut der Kristallplastizitat", Z. Phys., 61 (1930) pp. 767-781.

8. T. S Noggle and J. S. Koehler, "Electron Microscopy of Aluminum Crystals Deformed at Various Temperatures", J. Appl. Phys., 28 (1957) pp. 53-62.

9. J Diehl, S. Mader and A. Seeger, "Gleitmechanismus und Oberflachenerscheinungen bei kubisch flachenzentrierten Metallen, Z. Metallkunde, 46 (1955) pp. 650-657.

10. A Seeger, J. Diehl, S. Mader and R. Rebstock, "Work-Hardening and Work-Softening of Face-Centered Cubic Metal Crystals", Phil. Mag., 2 (1957) pp. 323-350.

11. S. Mader, "Elecktronenmikropische Untersuchung der Gleitinienbildung auf. Kupfereinkristallen", Z Physik, 149 (1957) pp. 73-103.

12. F. H. Blewitt, R. R. Coltman and J. K. Redman, "Work-Hardening in Copper Crystals", Report of a Conference on Defects in Crystalline Solids, Physical Society, London (1955) pp. 369-382.

13. N. F Mott, "A Theory of Work-Hardening of Metal Crystals", Phil. Mag., 43 (1952) pp. 1151-1178.

14. A H. Cottrell, "The Time Laws of Creep", J. Mech. and Phys. Solids, 1 (1952) pp. 53-63.

15. J Friedel, Les Dislocations, Ganthier-Villars, Paris, (1956).

16. A. Seeger, "Theorie der Kristallplastizitat," I. Grundzuge der Theorie, Z Naturforsch. 9A (1954) pp. 758-774; II. Die Grundstruktur der dichtest gepockten Metalle und ihr Einflass auf die plastische Verformung, Z. Naturforsch. 9A (1954) pp. 856-870; III. Die Temperatur- und Geschwindigkeitsabhangigkeit der Kristallplastizitat, Z. Naturforsch. 9A (1954) pp. 870-881; The Generation of Lattice Defects by Moving Dislocations and its Application to the Temperature Dependence of the Flow-Stress of F.C.C Crystals, Phil. Mag., 46 (1955) pp. 1194-1217.

17. N F Mott, "The Work-Hardening of Metals", 1960 Inst. of Metals Lecture, Trans. AIME, 218 (1960) pp. 962-968.

18. A N. Stroh, "Constrictions and Jogs in Extended Dislocations", Proc. Phys. Soc., London B (1954) pp. 427-436.

19. A. F. Kocks, "Polyslip in Single Crystals", Acta. Met., 8 (1960) pp. 345-352.

20. J. E. Bailey and P B. Hirsch, "The Dislocation Distribution, Flow-Stress, and Stored Energy in Cold-Worked Polycrystalline Silver", Phil. Mag., 5 (1960) pp. 485-497.

21. A H. Cottrell, "The Intersection of Gliding Screw Dislocations", Dislocations and Mechanical Properties of Crystals, John Wiley and Sons, Inc., New York (1957) pp. 509-512.

22. A. Seeger, S. Mader and K. Kronmuller, "Theory of Work-Hardening in F.C.C and H.C P. Single Crystals", Electron Microscopy and Strength of Crystals, Interscience, to be published.

23. S. K. Mitra and J E. Dorn, "On the Nature of Strain Hardening in Face-Centered Cubic Metals", Trans. AIME, to be published.

24. Z. S. Basinski, "Thermally Activated Glide in Face-Centered Cubic Metals and its Application to the Theory of Strain Hardening", Phil. Mag., 4 (1959) pp. 393-432.

25. V. G. Saada, Thesis, Faculty of Science, University of Paris, (1960).

26. G. Masing and J. Raffelsieper, "Mechanische Erholung von Aluminium-Einkristallen", Z. Metallk. 41 (1950) pp. 65-70.

27. K. Lucke and H. Lange, "Uber die Form der Verfestigungskurve von Reinstaluminium Kristallen und die Bildung von Deformationsbandern", Z. Metallk., 43 (1952) pp. 55-66.

28. F. D. Rossi, "Stress-Strain Characteristics and Slip-Band Formation in Metal Crystals: Effect of Crystal Orientation", Trans. AIME, 200 (1954) pp. 1009.

29. H. Suzuki, S. Ikeda, and S. Takeuchi, "Deformation of Thin Copper Crystals", J. Phys. Soc., Japan, 11 (1956) pp. 382-393.

30. H. Lange and K. Lucke, "Storungen der Gleitung bei Aluminium kristallen", I. Untersuchung der Verfestigung und des Laue-Asterismus, Z. Metallk. 44 (1953) pp. 183-191; II. Mikroskopische Untersuchung des Gleitlinienbildes und Diskussion des Verformungsmechanisms, Z. Metallk. 44 (1953) pp. 514-527.

31. B. Chalmers, "The Plasticity of Polycrystalline Solids", Plastic Deformation of Crystalline Solids, Mellon Inst., Pittsburgh (1950) pp. 193-196.

32. J. D. Livingston and B. Chalmers, "Multiple Slip in Bicrystal Deformation", Acta Met., 5 (1957) pp. 322-327.

33. R. L. Fleischer and W. A. Backofen, "Effects of Grain Boundaries in Tensile Deformation at Low Temperatures", Trans. AIME, 218 (1960) pp. 243-251.

34. K. J. Aust and N. K. Chen, "Effect of Orientation Difference on the Plastic Deformation of Aluminum Bicrystals", Acta Met., 2 (1954) pp. 632-638.

35. R. Clark and B. Chalmers, "Mechanical Deformation of Aluminum Bicrystals", Acta Met., 2 (1954) pp. 80-86.

36. C. Elbaum, "Plastic Deformation of Aluminum Multicrystals", Trans. AIME, 218 (1960) pp. 444-448.

37. F. D. Rossi and C. H. Mathewson, "A Study of the Plastic Behavior of High-Purity Aluminum Single Crystals at Various Temperatures", Trans. AIME, 188 (1950) pp. 1159-1167.

38. R. J. Hartman and E. Macherauch, "Unterschung von Gleitvorgangen in Einzelkristalliten vielkristalliner Kupferproblem", Z. Metallk., 51 (1960) pp. 694-699.

39. S. K. Mitra, P. W. Osborne and J. E. Dorn, "On the Intersection Mechanism of Plastic Deformation in Aluminum Single Crystals", Trans. AIME, 221 (1961) pp. 1206-1213.

40. R. V. Mises, "Mechanik der Plastischen Formanderung von Kristallen", Z. ang. Math. und Mech., 8 (1928) pp. 161-185.

41. G. Sachs, "Zur Ableitung einer Fliessbedingung", Z. d. Ver. deut. Ing., 72 (1928) pp. 734-736.

42. H. L. Cox and D. G. Sopwith, "Effect of Orientation on Stresses in Single Crystals and of Random Orientation on Strength of Polycrystalline Aggregates", Proc. Phys. Soc., 49 (1937) pp. 134-151.

43. A. Kochendorfer, Plastische Eigenschaften von Kristallen, Springer, Berlin (1941).

44. E. A Calnan and C. J. B. Clews, "Deformation Textures in Face-Centered Cubic Metals", Phil. Mag., 41 (1950) pp. 1085-1100.

45. S. B. Batdorf and B. Budiansky, "A Mathematical Theory of Plasticity Based on the Concept of Slip", NACA Tech. Note No. 1871.

46. G. I Taylor, "Plastic Strain in Metals", J. Inst. Met., 62 (1938) pp. 307-324; "Analysis of Plastic Strain in a Cubic Crystal", Stephen Timoshenko 60th Anniv. Vol, pp. 218-224; "Strains in Crystalline Aggregates", Deformation and Flow of Solids, Madrid (1955) pp. 3-12.

47. J. F. W. Bishop and R. Hill, "A Theory of the Plastic Distortion of a Polycrystalline Aggregate under Combined Stresses", Phil. Mag., 42 (1951) pp. 414-427. "A Theoretical Derivation of the Plastic Properties of a Polycrystalline Face-Centered Metal", Phil. Mag., 42 (1951) pp. 1298-1307.

48. J. F. W. Bishop, "A Theoretical Examination of the Plastic Deformation of Crystals by Glide", Phil. Mag., 44 (1953) pp. 51-64.

49. W. Boas and M. E. Hargreaves, "On the Inhomogenelty of Plastic Deformation in the Crystals of an Aggregate", Proc. Roy. Soc., A 193 (1948) pp. 89-97.

50. V. M. Urie and H. L. Wain, "Plastic Deformation of Coarse-Grained Aluminum", J. Inst. Metals, 81 (1952-1953) pp. 153-159.

51. R. C Deshpande, "Inhomogeneous Deformation in Polycrystalline Metals", Trans. Indian Inst. of Metals, 13 (1960) pp. 241-248.

52. C. S. Barrett and L H. Levenson, "The Structure of Aluminum after Compression", Trans. AIME, 137 (1940) pp. 112-126.

53. J. F. W. Bishop, "A Theory of the Tensile and Compressive Textures of Face-Centered Cubic Metals", J. Mech. and Phys. Solids, 3 (1954) pp. 130-142.

54. U. F. Kocks, "Polyslip in Polycrystals", Acta Met., 6 (1958) pp. 85-94.

55. S. Howe and C. Elbaum, "The Relation between the Plastic Deformation of Aluminium Single Crystals and Polycrystals", Phil. Mag., 6 (1961) pp. 37-48.

56. J. E. Dorn, P. Pietrokowsky and T. E. Tietz, "The Effect of Alloying Elements and the Plastic Properties of Aluminum Alloys", Trans. AIME, 188 (1950) pp 933-943.

57. R. A. Wilkins and E. S. Bunn, Copper and Copper Base Alloys, McGraw-Hill Book Co., Inc., New York, 1943.

58. C. Zener, "A Theoretical Criterion for the Initiation of Slip Bands", Phys. Rev., 69 (1946) pp. 128-129.

59. J. S. Koehler, "On the Dislocation Theory of Plastic Deformation", Phys. Rev., 60 (1941) pp. 397-410.

60. J. D. Eshelby, F. C. Frank and F. R. N Nabarro, "The Equilibrium of Linear Arrays of Dislocations", Phil. Mag., 42 (1951) pp. 351-364.

61. A. N. Stroh, "The Formation of Cracks as a Result of Plastic Flow", Proc. Roy. Soc., 223 (1954) pp. 404-414; "A Theory of Fracture of Metals", Advances in Physics, 6 (1957) pp. 418-465.

62. D. A. Thomas and B. L. Averbach, "The Early Stagesof Plastic Deformation in Copper", Acta Met., 7 (1959) pp. 69-75.

63. N. Brown and K. F. Lukens, Jr., "Microstrain in Polycrystalline Metals", Acta Met., 9 (1961) pp. 106-111.

64. Budiansky, Z. Hashin and J. S. Sanders, Jr., "The Stress Field of a Slipped Crystal and the Early Plastic Behavior of Polycrystalline Materials", Plasticity, Proc. of Second Symposium on Naval Structural Mechanics, Pergammon Press, London, 1960.

65. J D. Eshelby, "The Determination of the Elastic Field of an Ellipsoidal Inclusion and Related Problems", Proc. Roy. Soc., A 241 (1957) pp. 376-396.

66. E. Kroner, "Zur Plastischen Verformung Des Vielkristalls", Acta Met., 9 (1961) pp. 155-161.

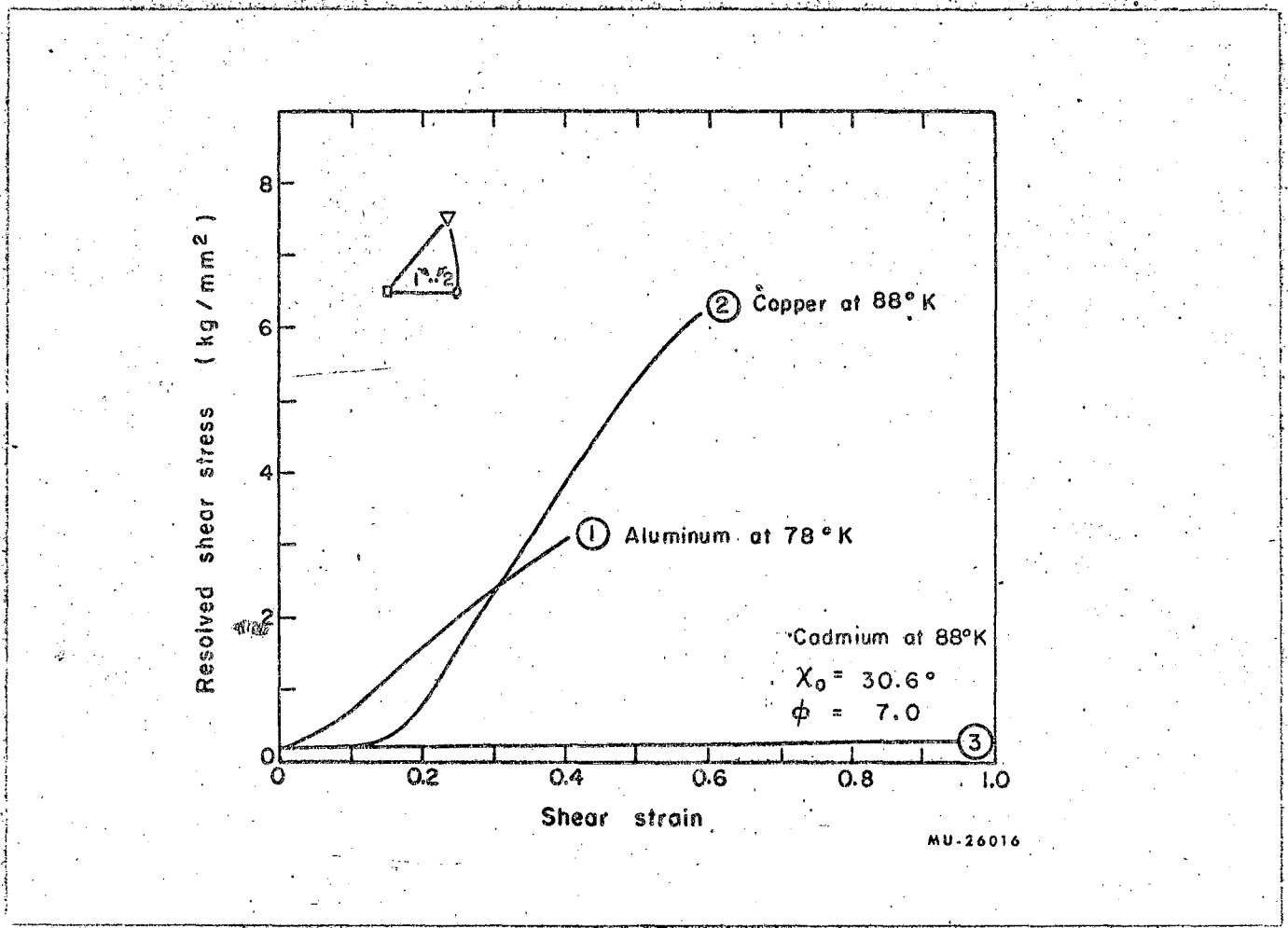

Fig. 1 Shear-stress vs Shear-strain Curves for Cd,[7] Al,[8] and Cu[9] Single Crystals of Similar Orientation

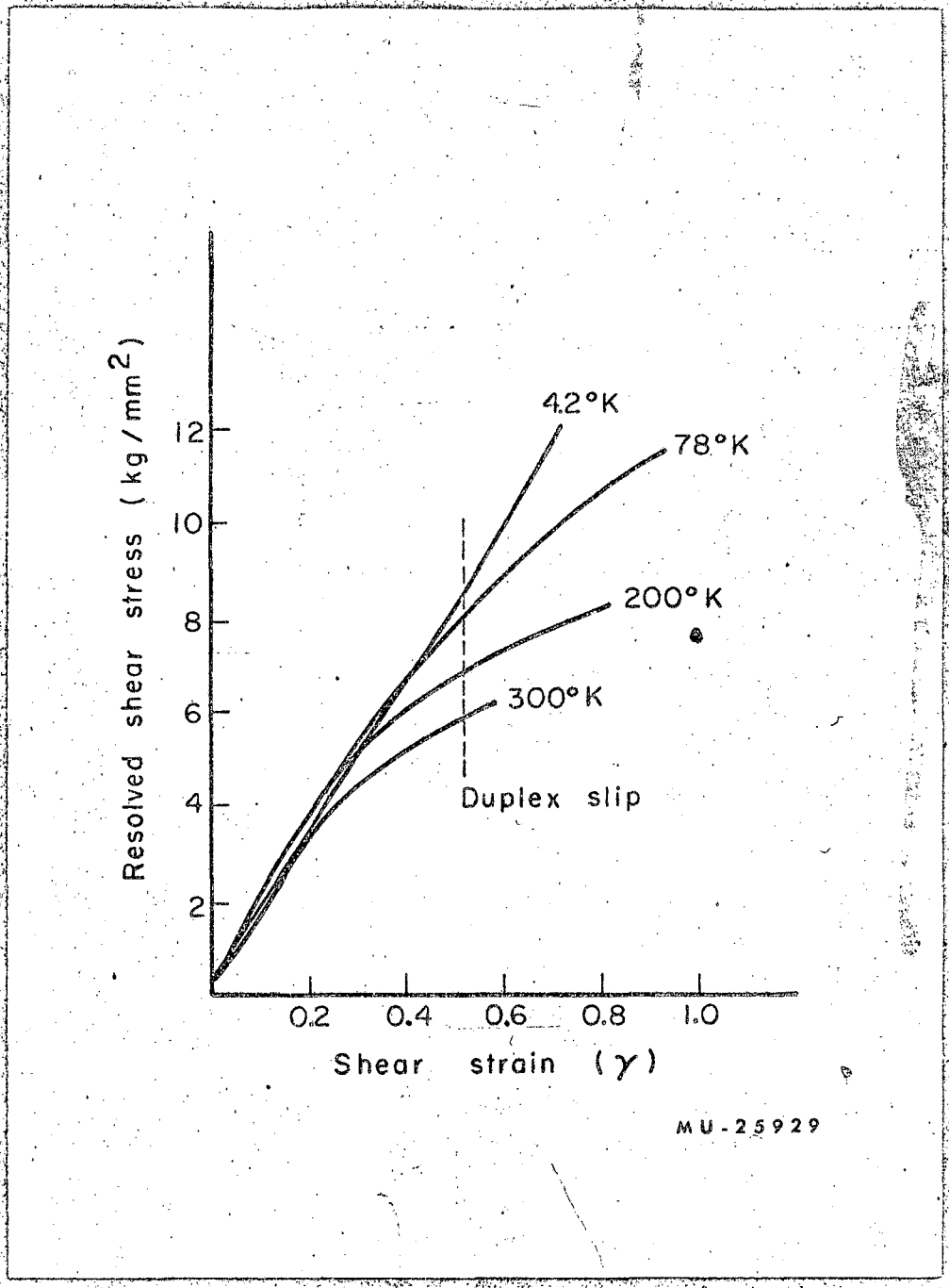

Fig. 2 Influence of Temperature on the Stress, τ_{II}, τ_{III} for Crystals of Cu of Identical Orientation.[12]

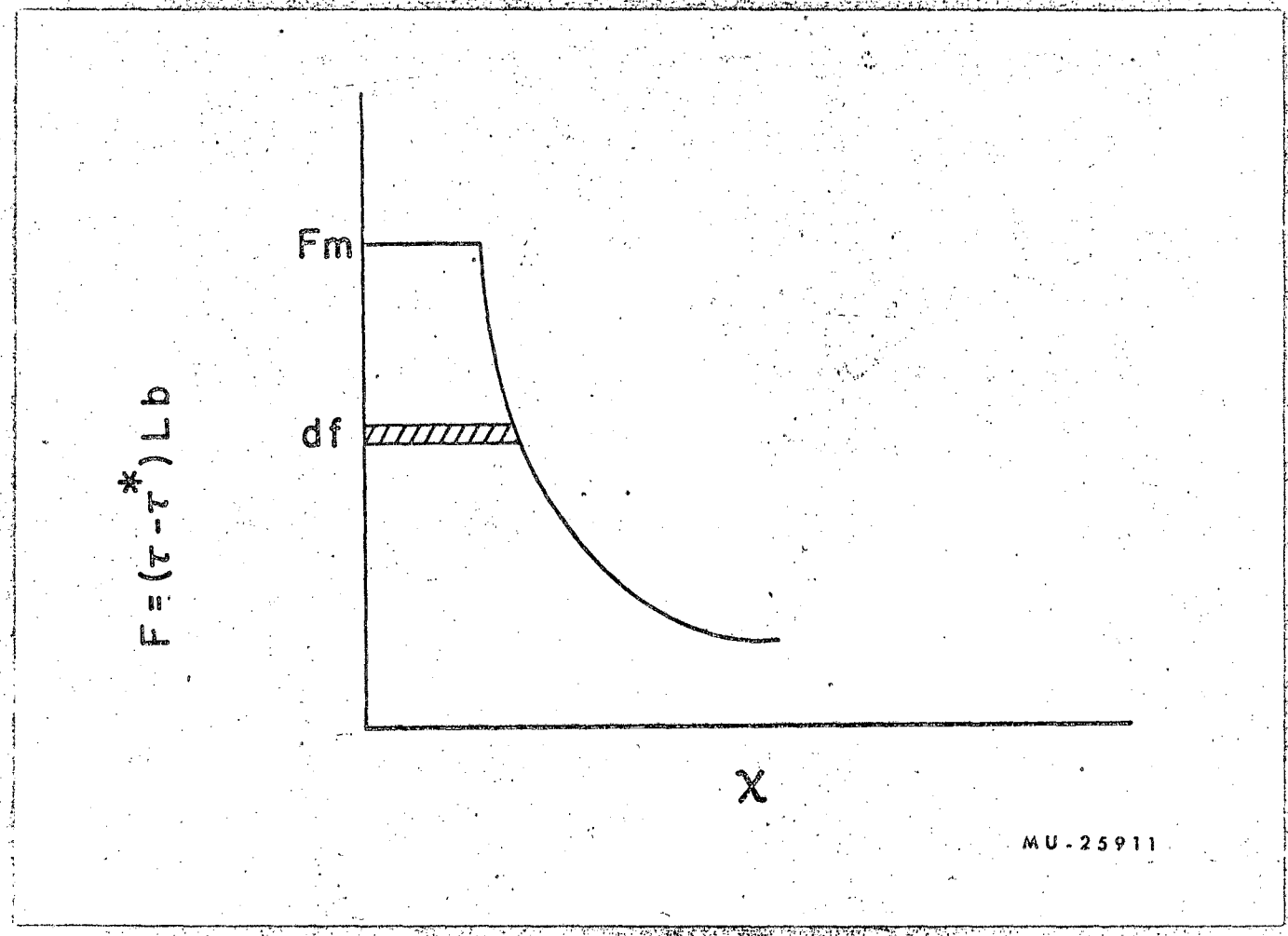

Fig. 3 Force vs Displacement Diagram for Activation Slip

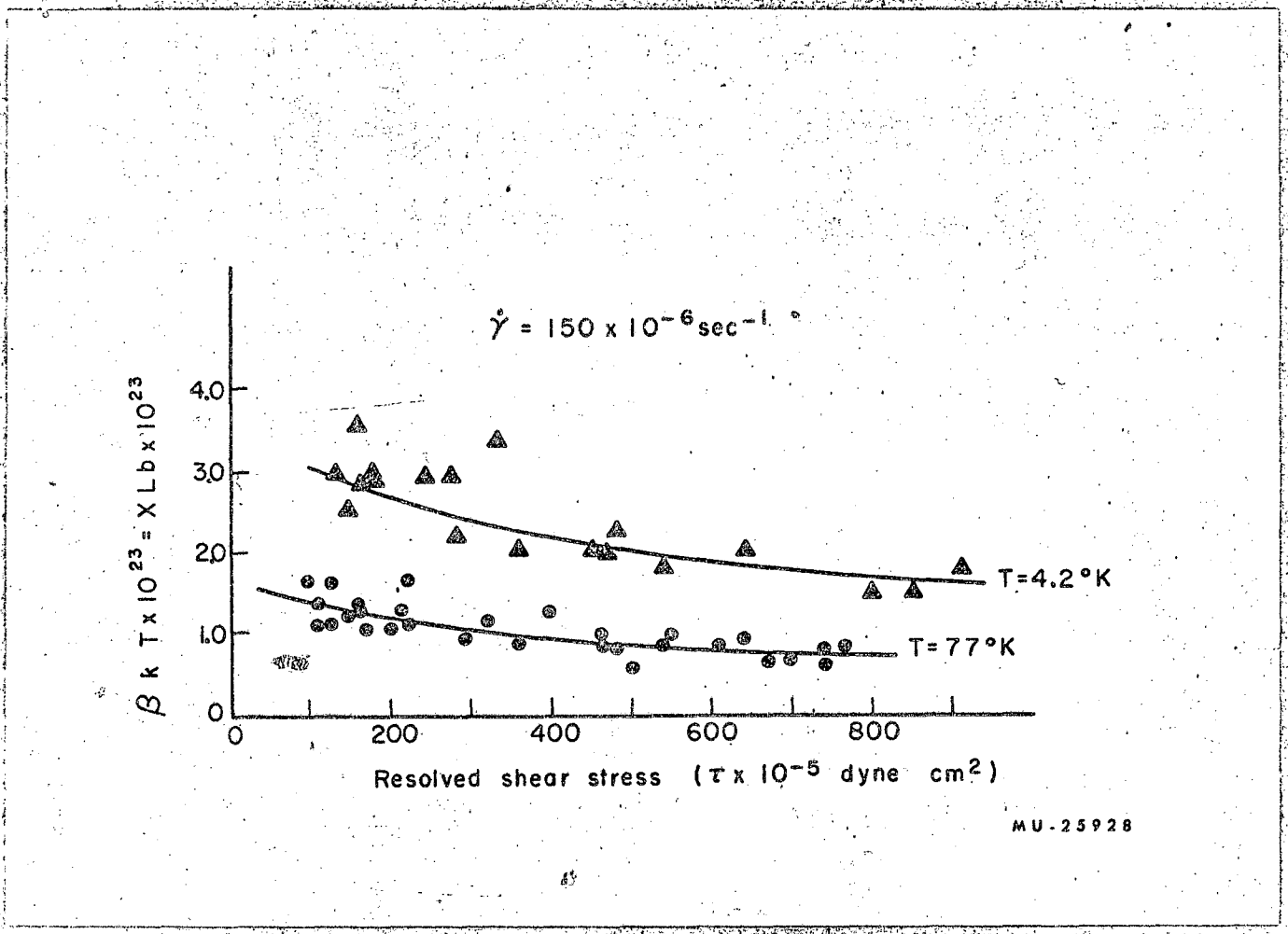

Fig. 4 Activation Volume vs Resolved Shear Stress for Cu Single Crystals at 4.2 and 77°K. (23)

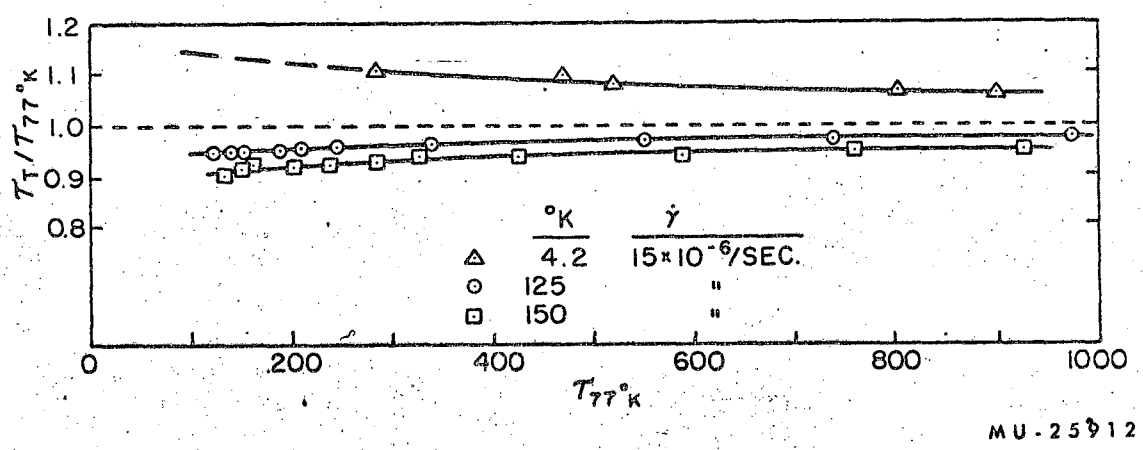

Fig. 5 Cottrell-Stokes Ratio τ_T/τ_{77} vs τ_{77} at Various Temperatures, T, for Cu Single Crystals. (23)

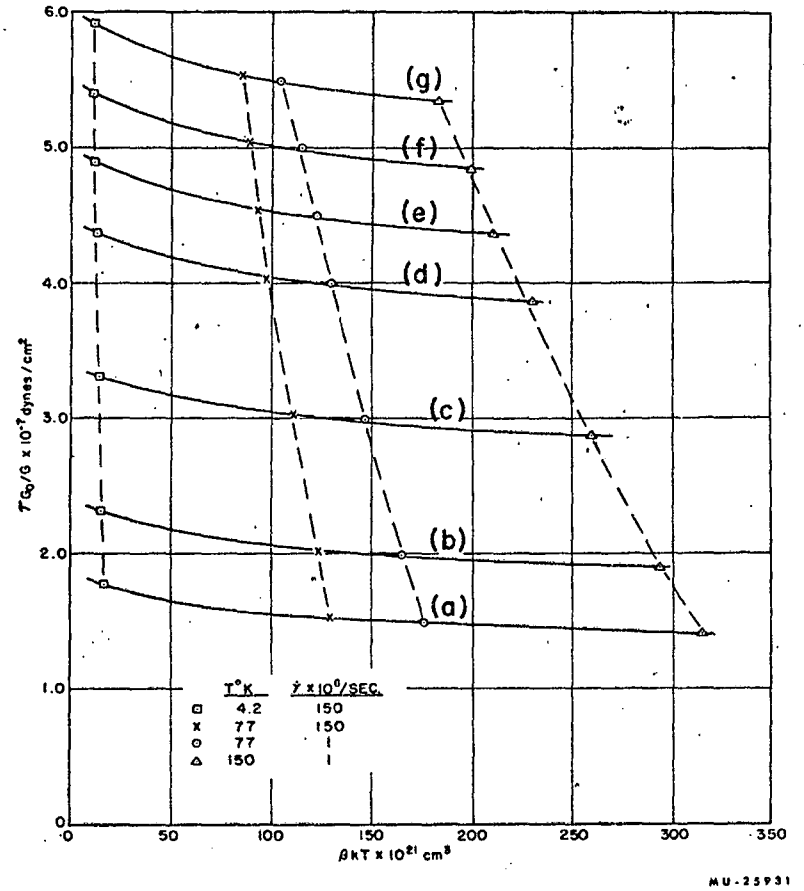

Fig. 6 $\tau G_0/G$ vs βkT for Different Values of Strain Adjusted to $\dot{\gamma}^0 = 15 \times 10^{-6}/\text{sec}^{-1}$ for Cu Single Crystals

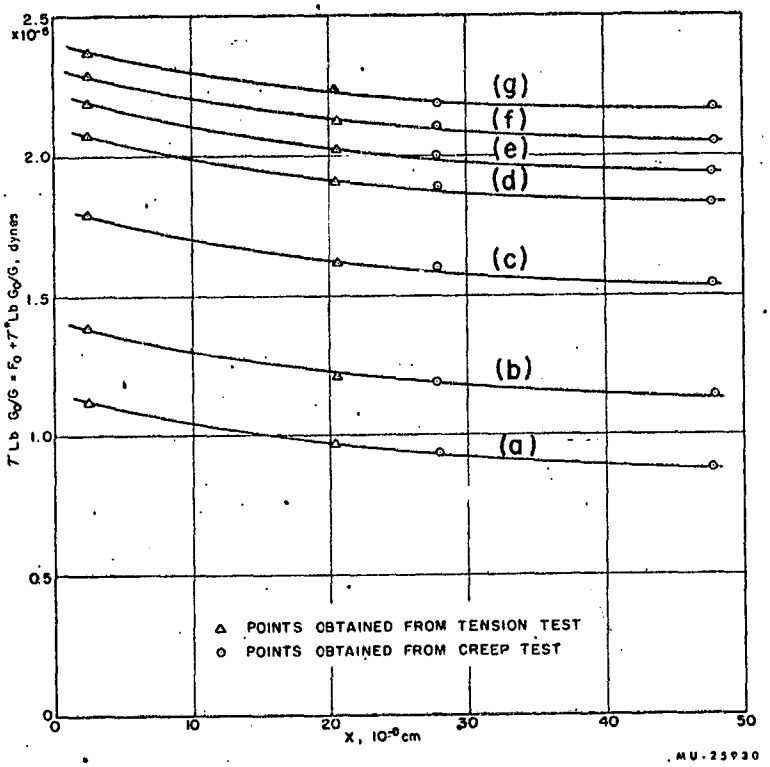

Fig. 7 $\tau Lb G_o/G$ vs χ for Cu Single Crystals.[23]

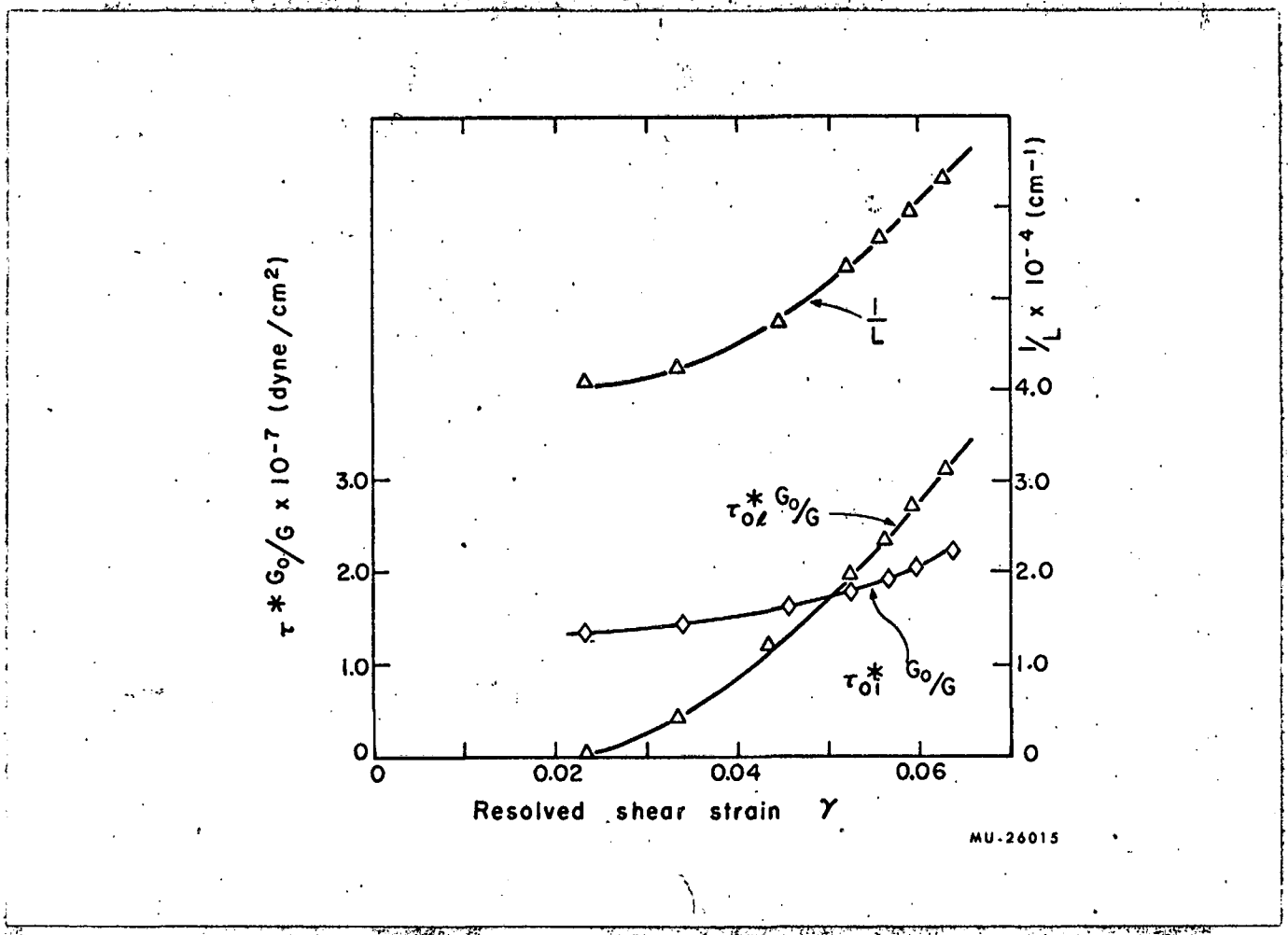

Fig. 8 Variation of $\tau_{o\ell}^*$, τ_{oi}^* and $\frac{1}{L}$ with Strain for Cu Cu Single Crystals.[23]

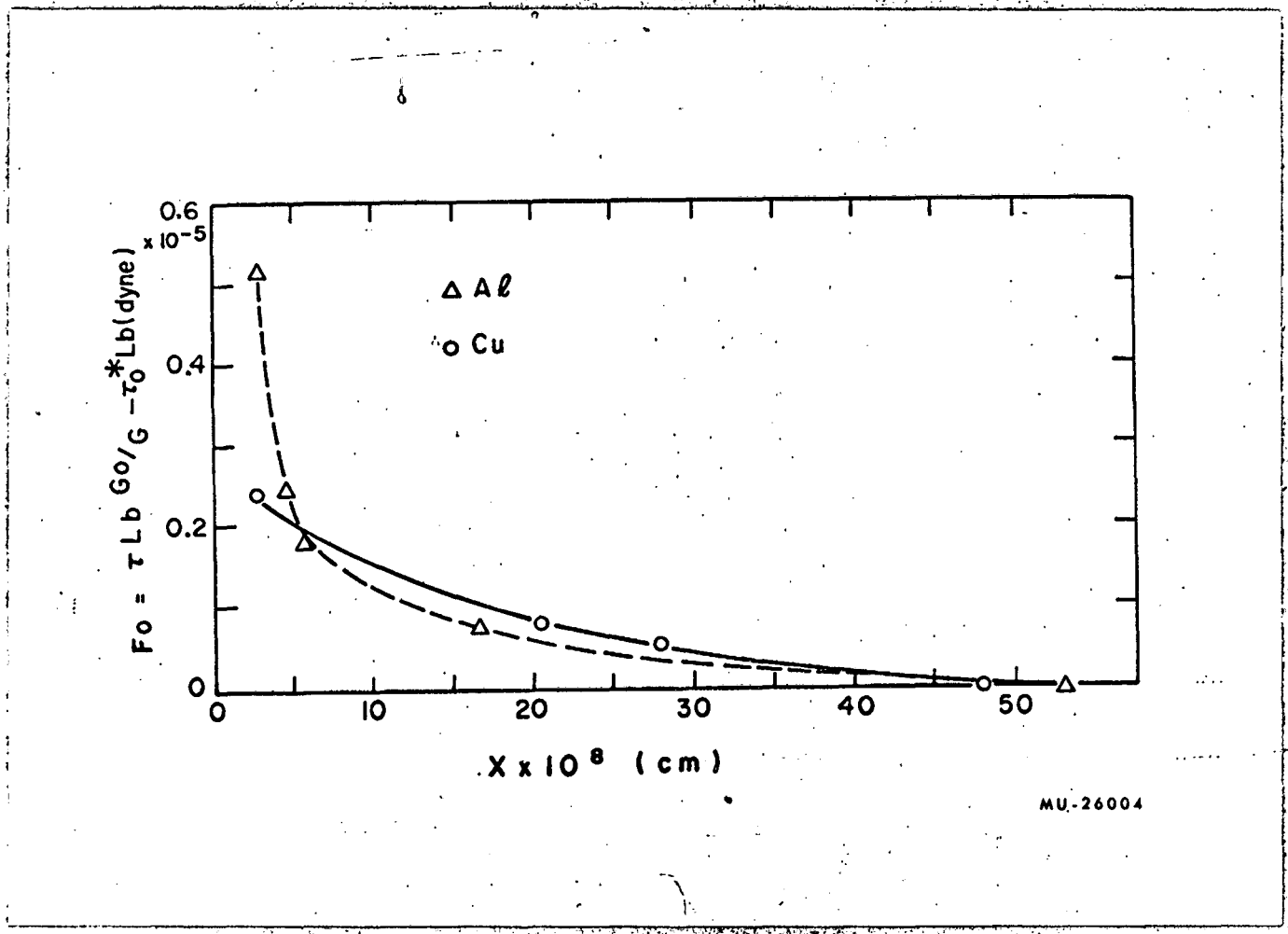

Fig. 9 F_o vs χ diagram for Cu and Al Single Crystals.[23]

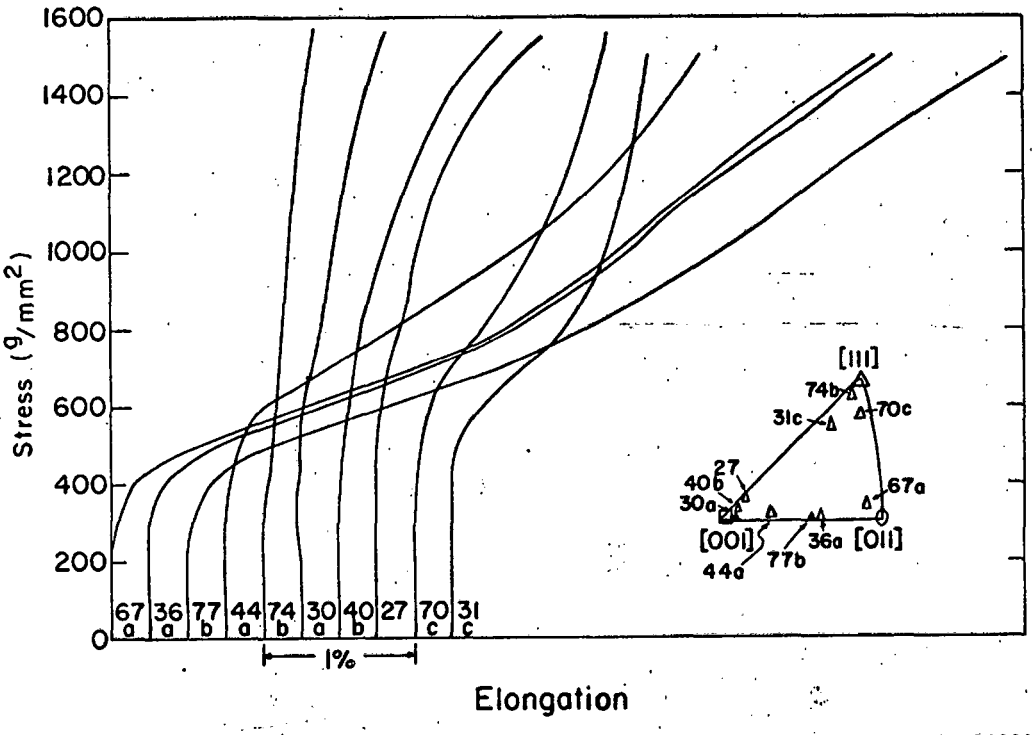

Fig. 10 Effect of Orientation on the Stress vs Displacement Curves for Single Crystals of Al. (26, 27)

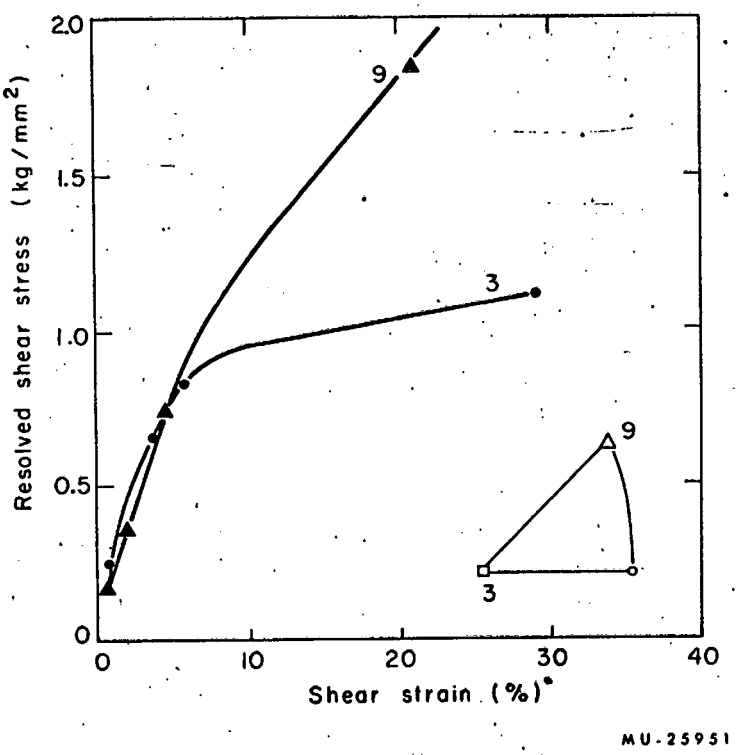

Fig. 11 Comparison of the Rates of Strain Hardening for Crystals Axes Near the [111] and [001] Pole.(30)

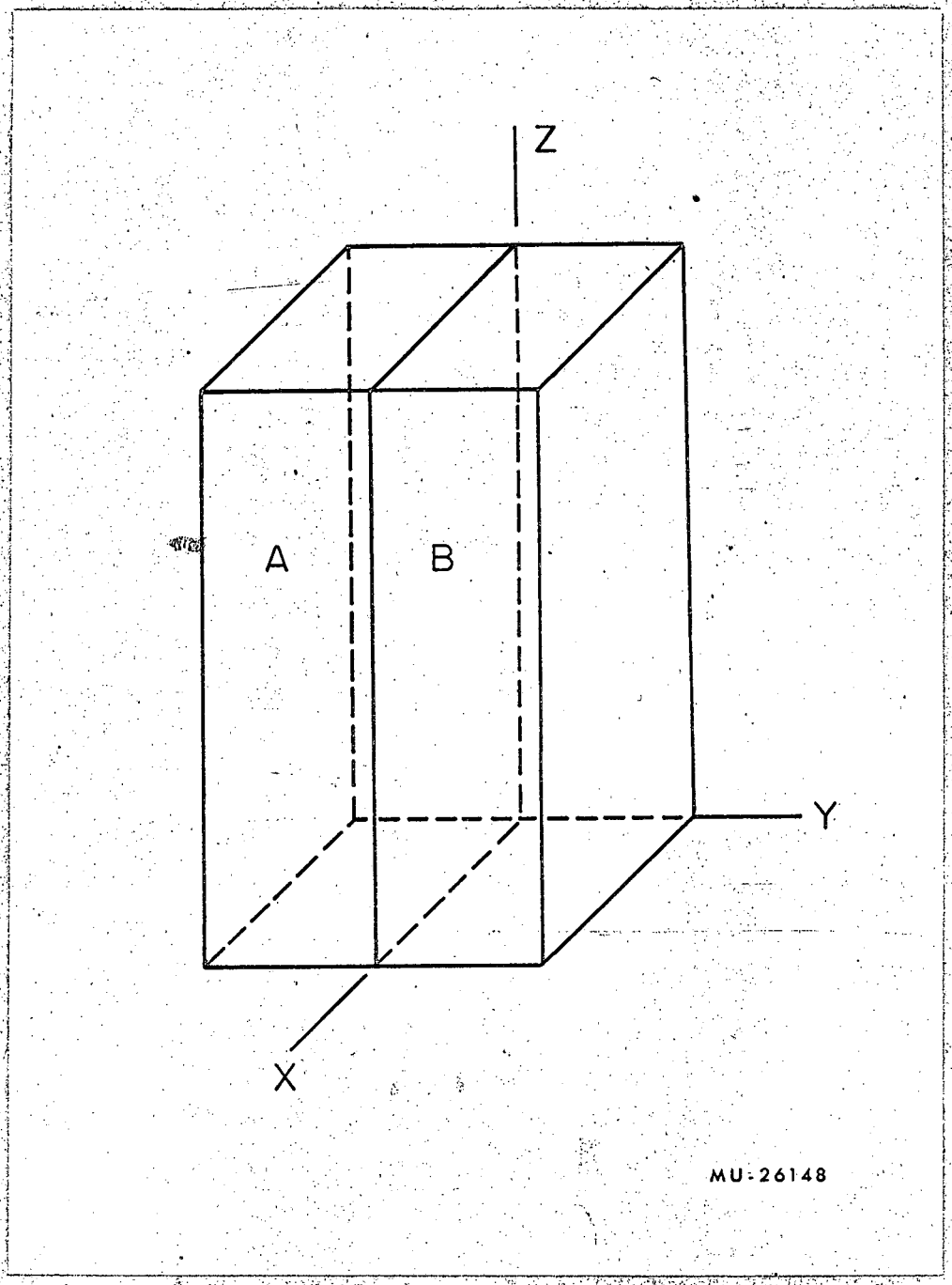

Fig. 12 Schematic Diagram of Bicrystals

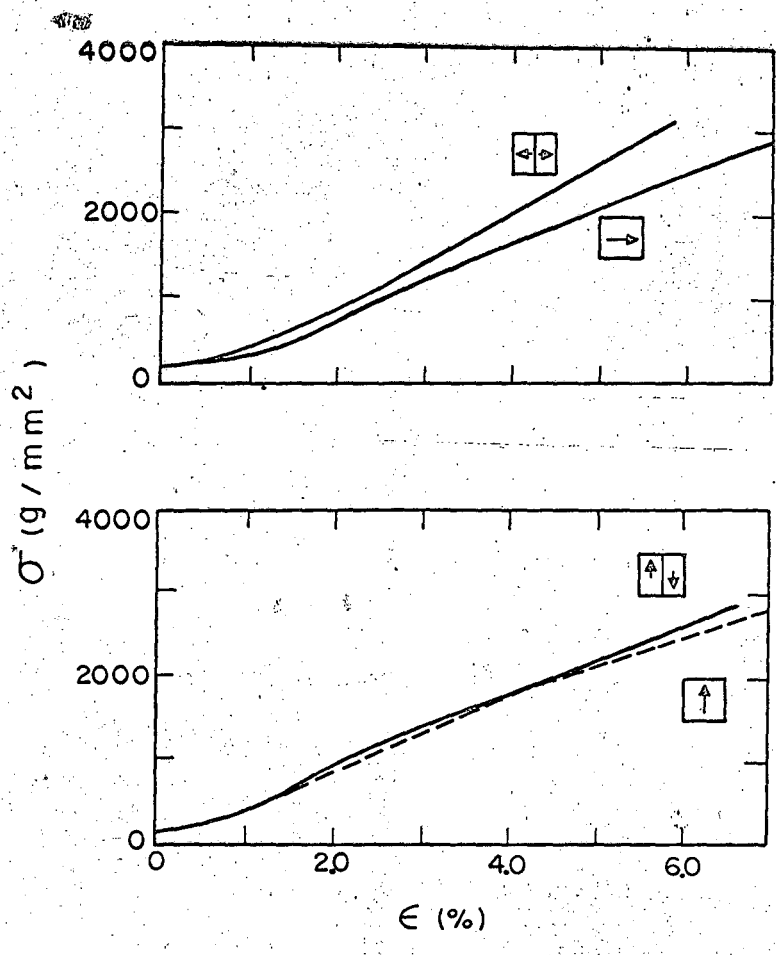

Fig. 13 Comparison of Single Crystal and Compatible Bicrystal Stress vs Strain Curves. (33)

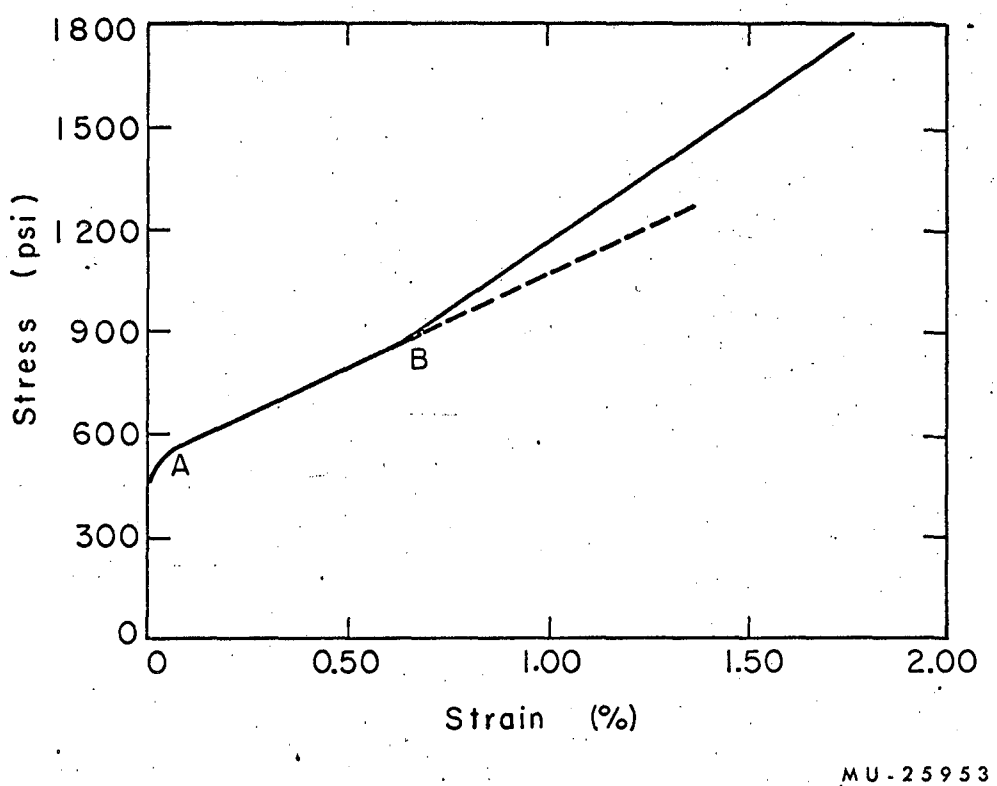

Fig. 14 Typical Stress vs Strain Curve for Aluminum Bicrystal with $\theta = 85^{\circ}$. (34)

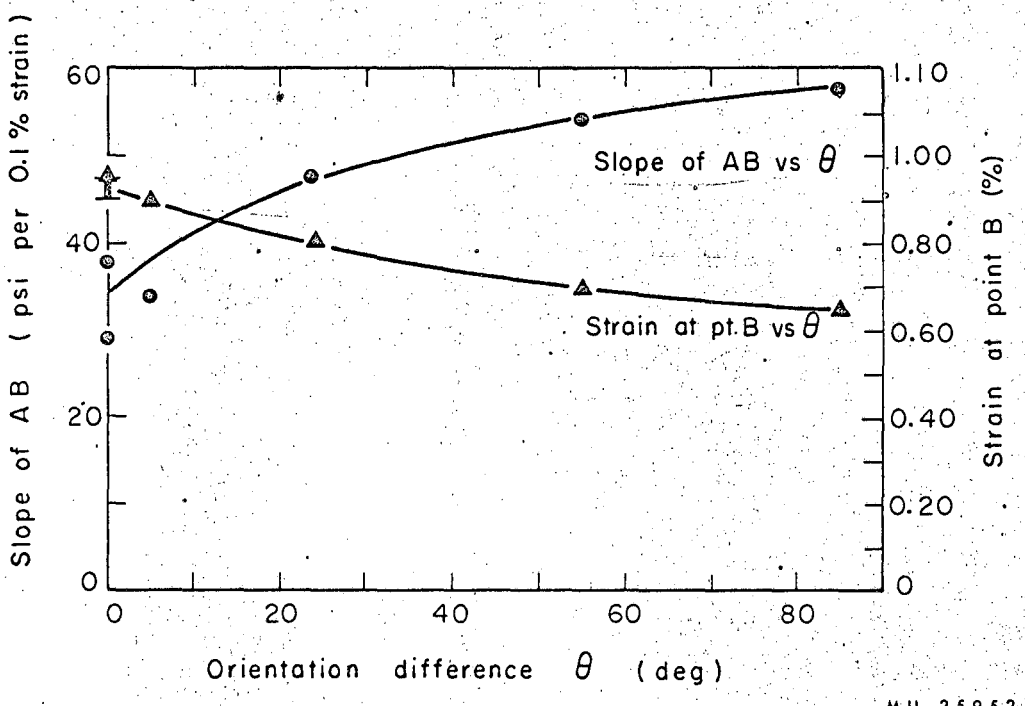

Fig. 15 Rate of Work-hardening and Strain to Initiation of Rapid Work-hardening vs Orientation.[34]

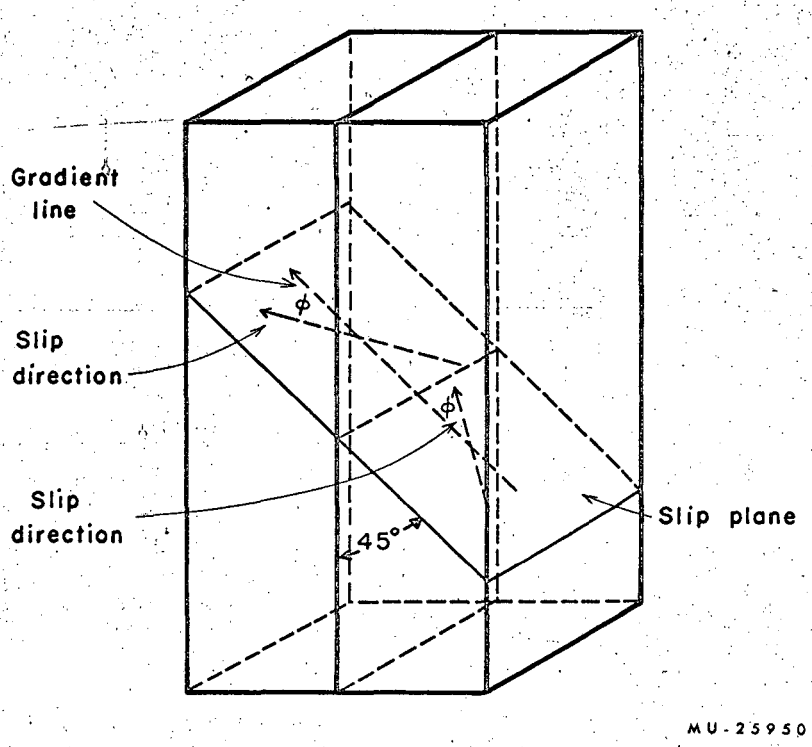

Fig. 16 Schematic of Bicrystals with Coplanar (111) Planes.

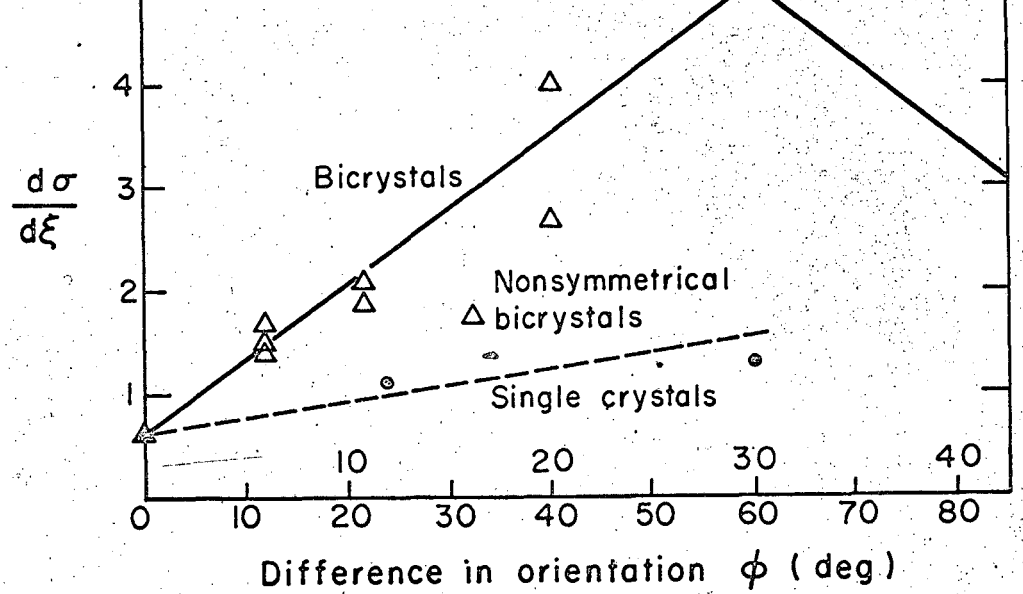

Fig. 17 Rate of Work-hardening vs Orientation. (35)

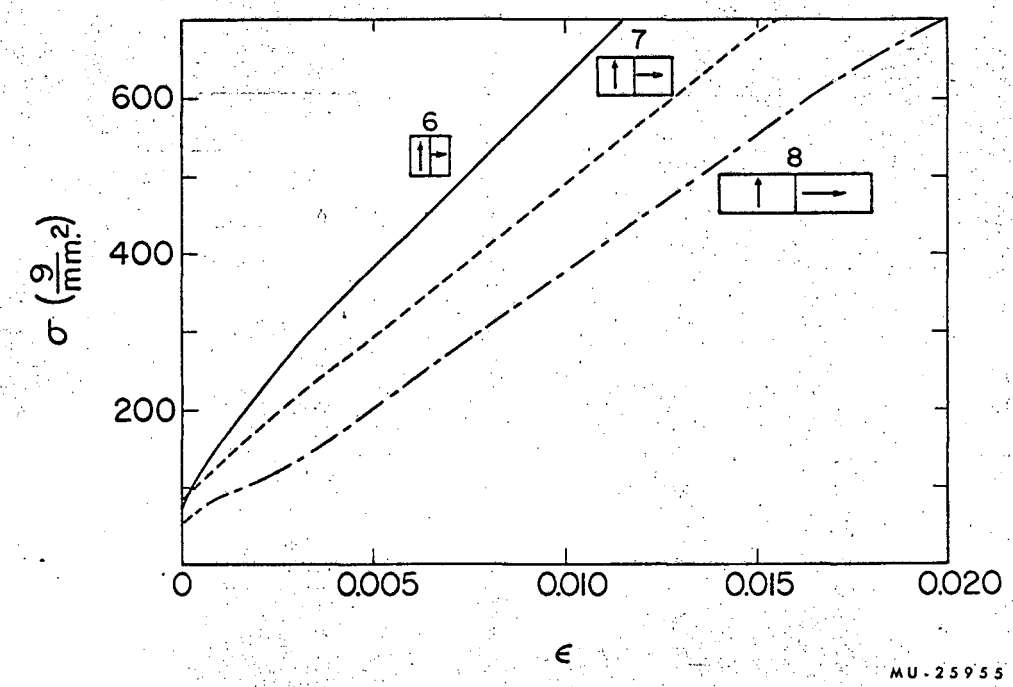

Fig. 18 Grain Boundary Size Effects: Deformation of Bicrystals of Three Widths

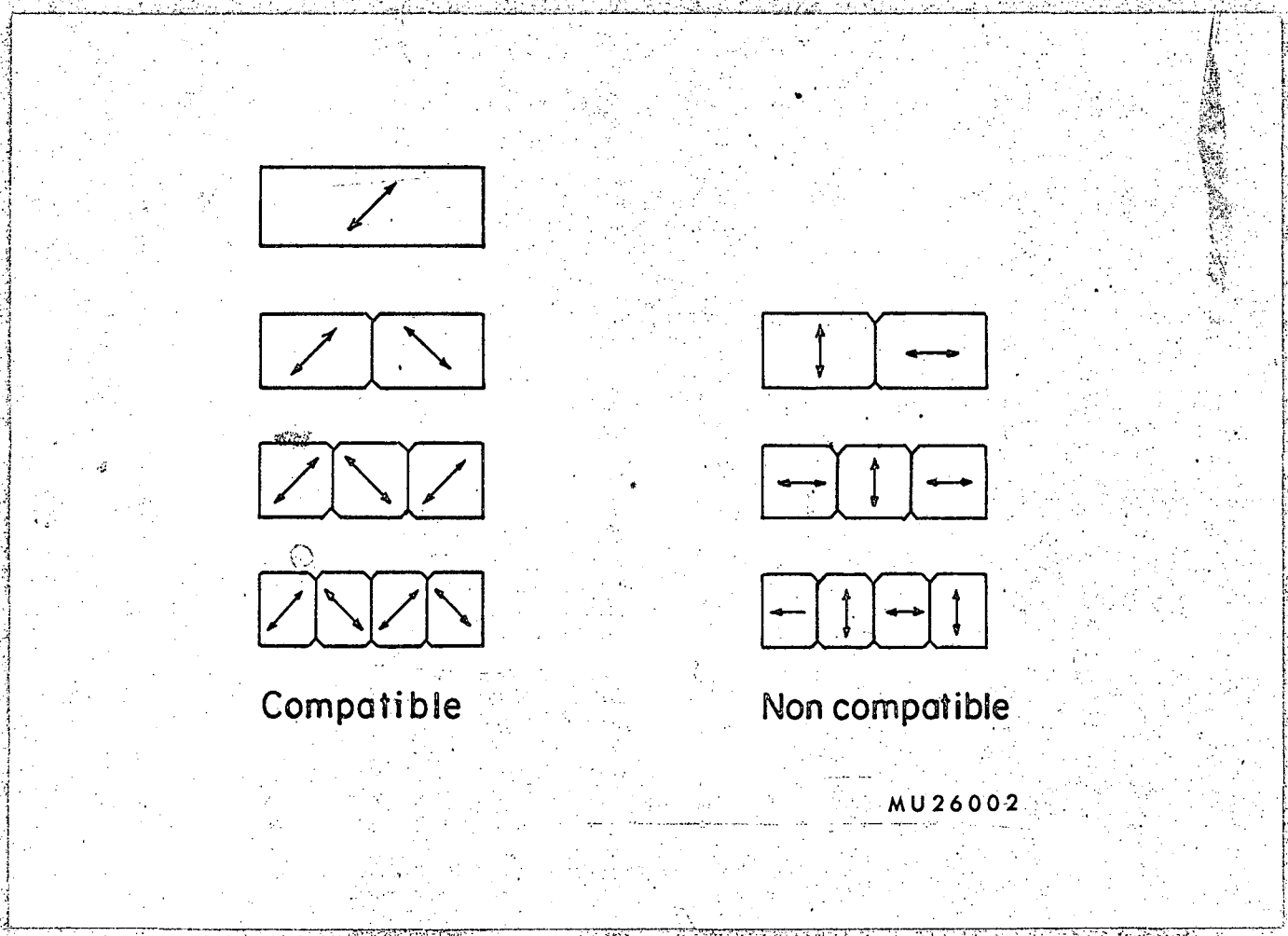

Fig. 19 Isoaxial Orientations of Single Bi-, Tri- and Quadru-crystals. (36)

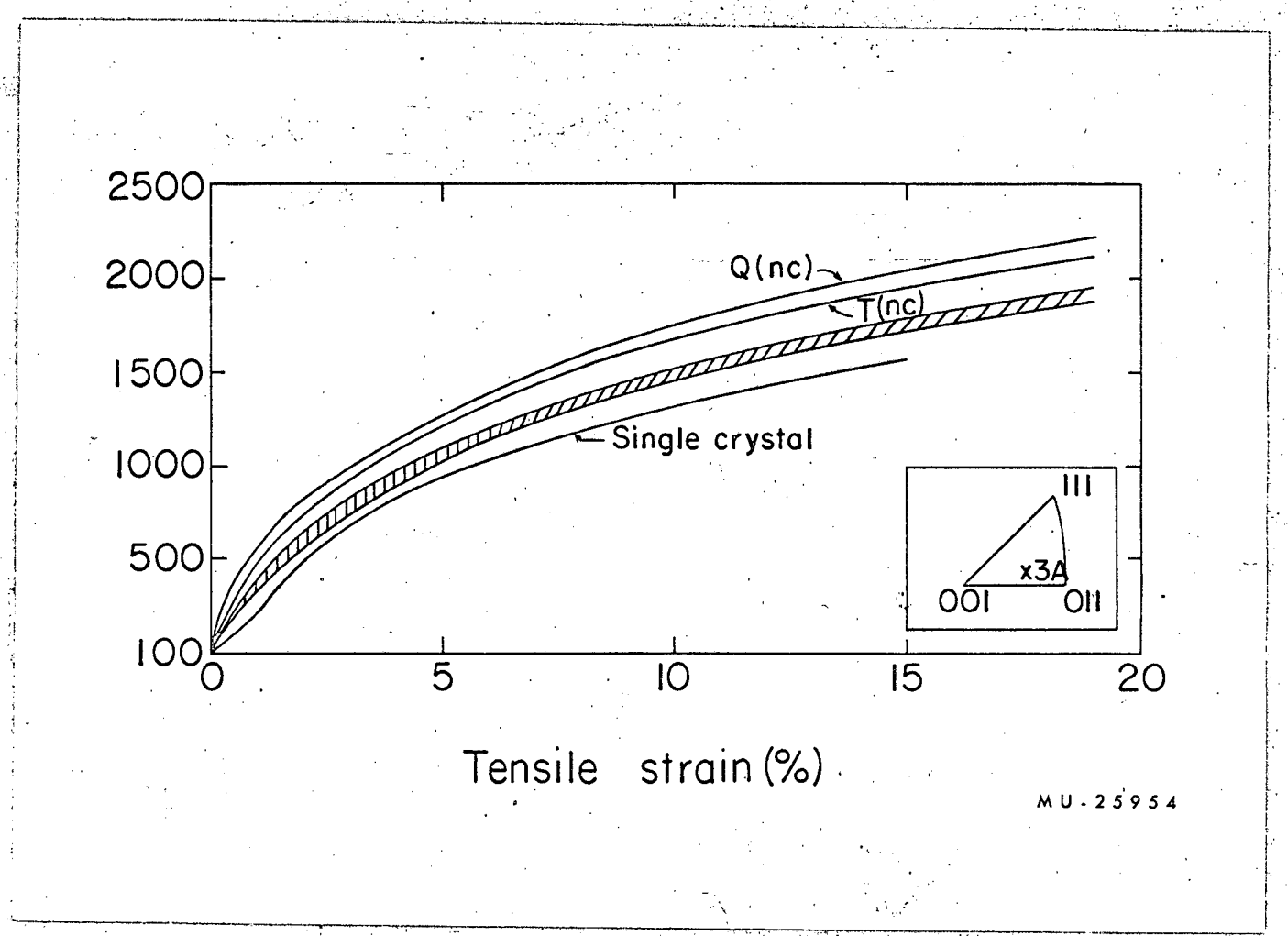

Fig. 20 Stress vs Strain Curves for Multi-crystals (Q (nc) ≡ non-compatible quadru-crystal. T (nc) ≡ non-compatible tri-crystal. Shaded area includes compatible bi-, tri-, and quadru-crystals plus non-compatible bicrystals.)

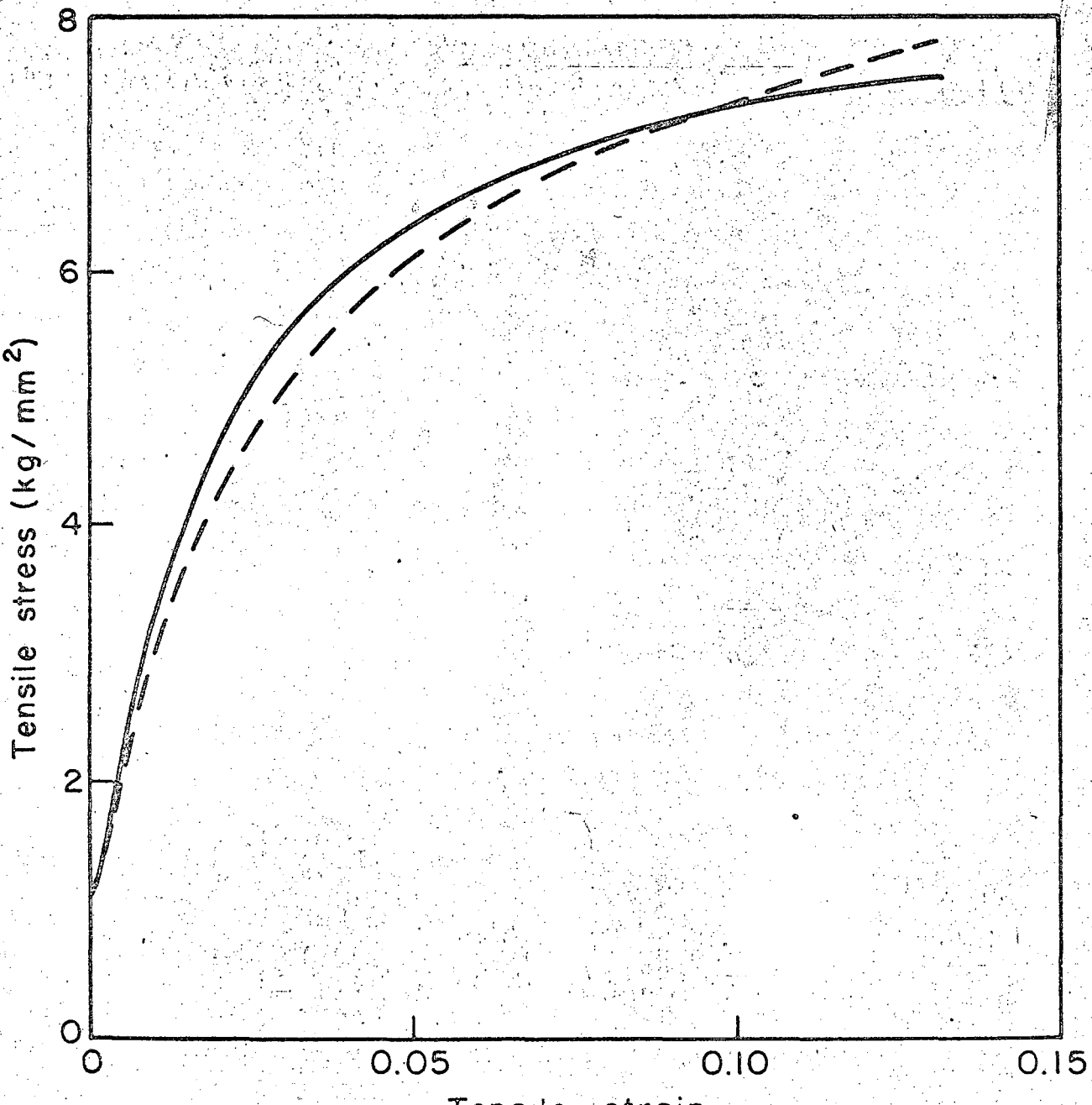

Fig. 21 Stress vs Strain Curves for Polycrystals of 99.5% Al: Experimental (————) and Theoretical (— — — —). (54, 27)

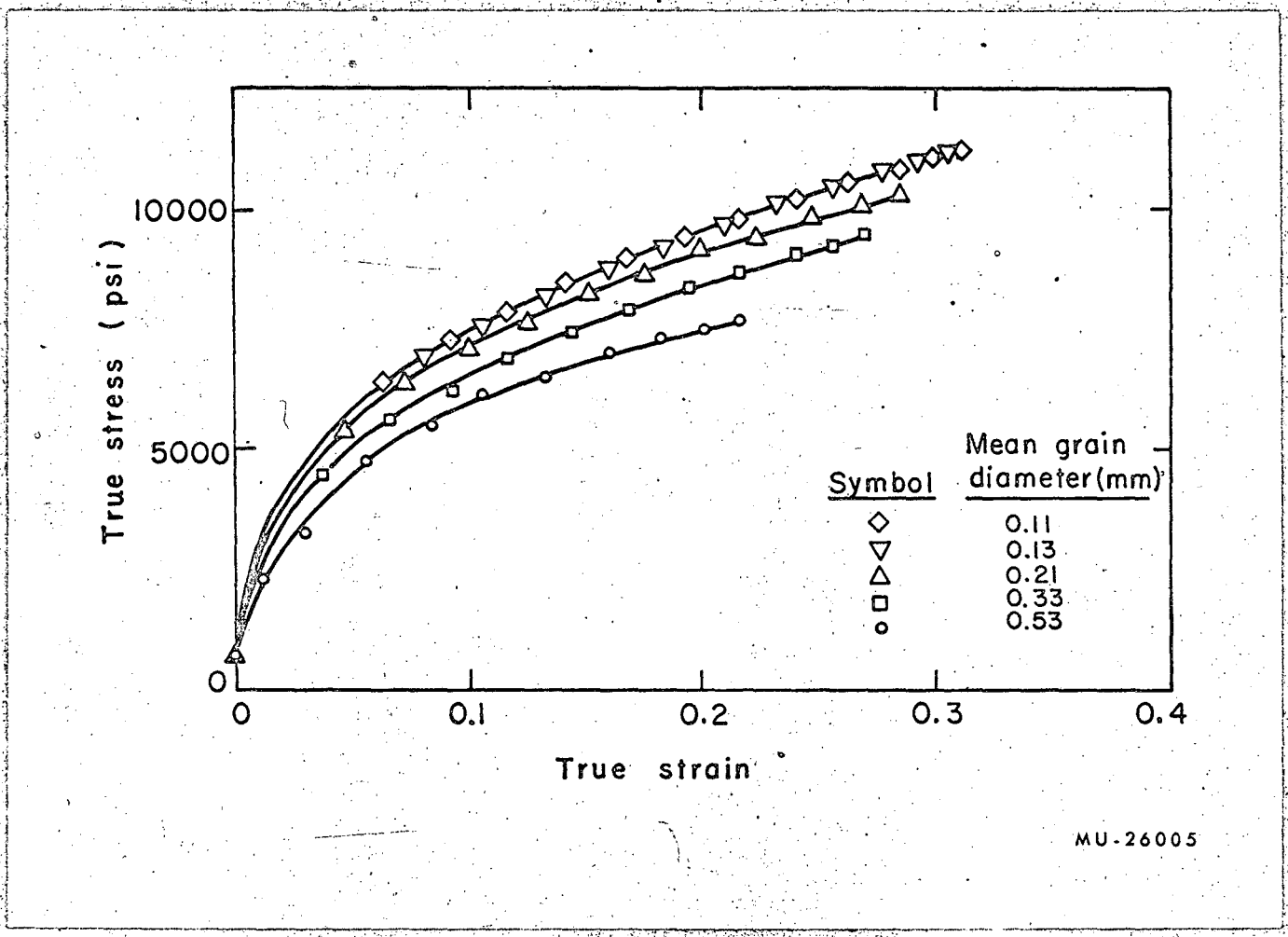

Fig. 22 Stress vs Strain Curves of Polycrystalline Aluminum for Various Grain Sizes. (56)

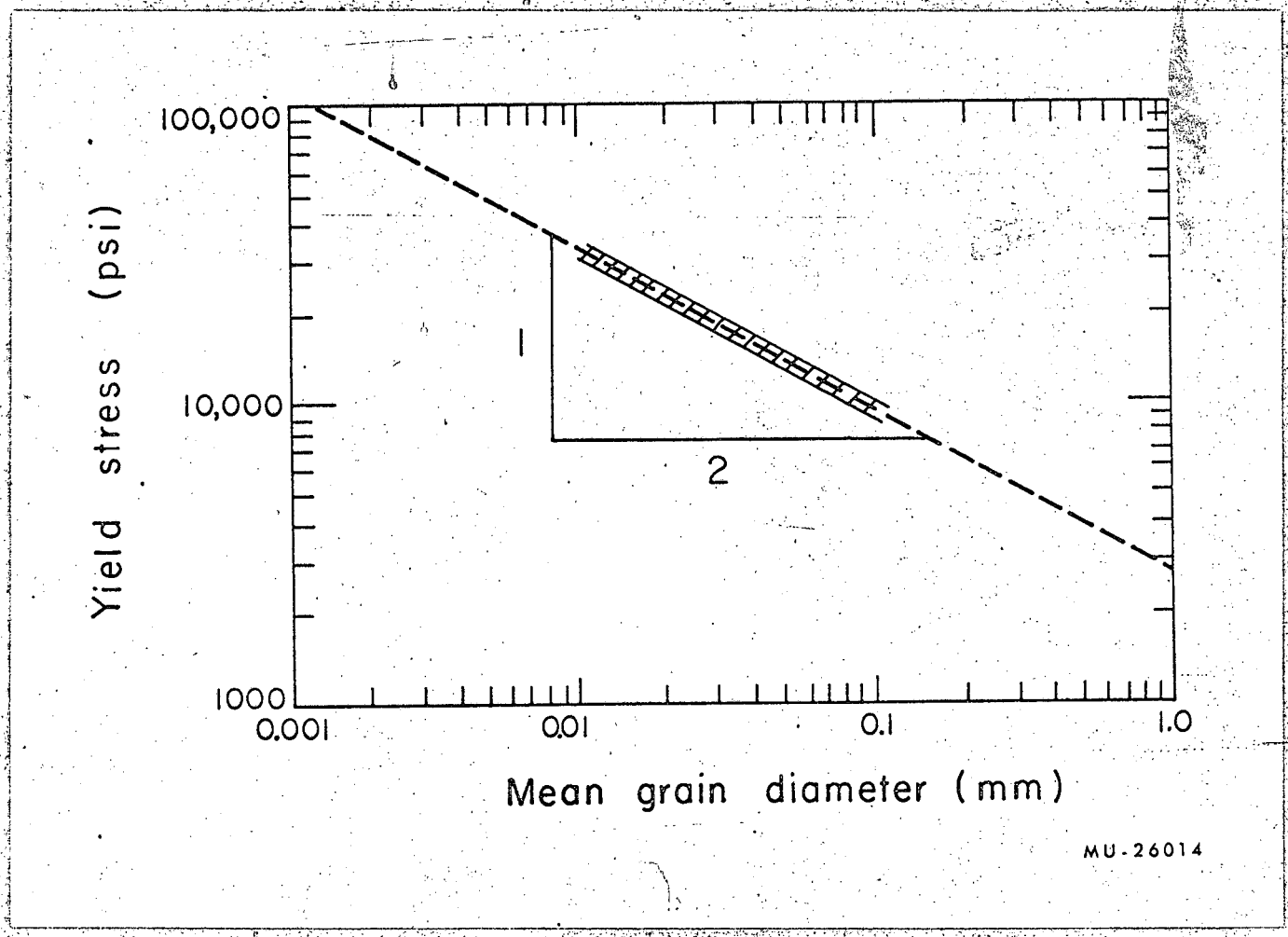

Fig. 23 Effect of Grain Size on Yield Strength for Cu and Cu Alloys.[57, 58]

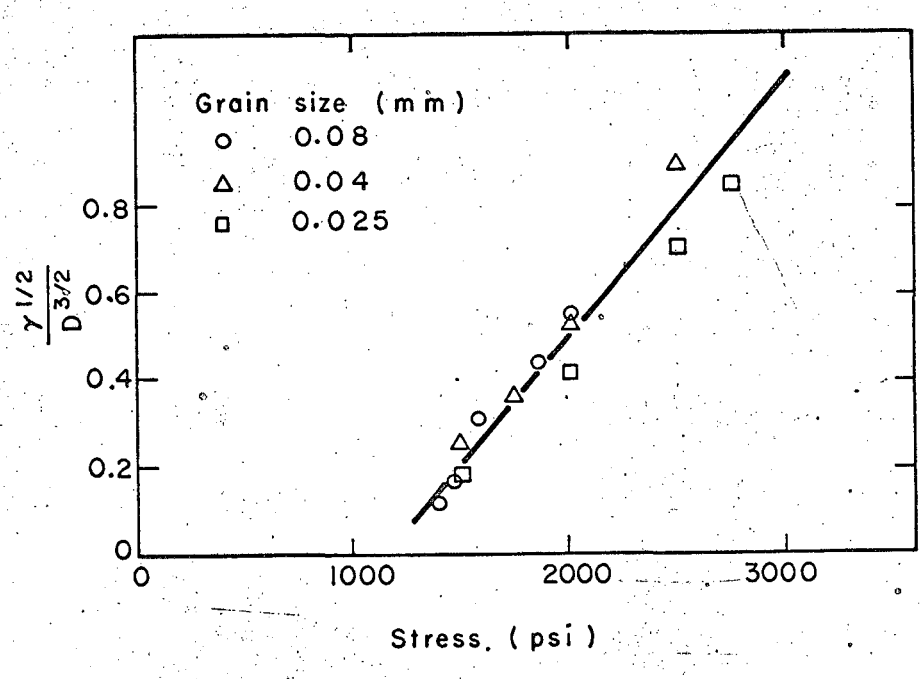

Fig. 24 $\frac{\gamma_e^{1/2}}{D^{3/2}}$ vs Stress. (63)

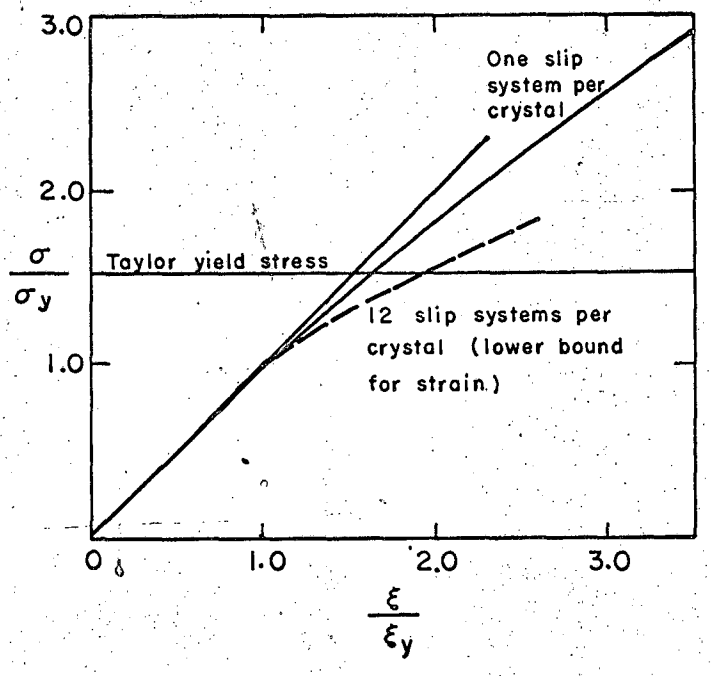

Fig. 25 σ/σ_y vs $\varepsilon/\varepsilon_y$ (64)